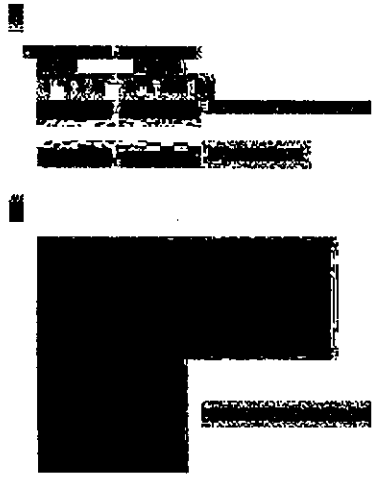

FIG. 9. **The phosphorylation of CREB is regulated by Ca^{2+} modulators in H9c2 cells.** *A*, H9c2 cells were incubated with thapsigargin (5 μM) or BAPTA-AM (10 μM) for the periods indicated, then cell extracts were prepared. The phosphorylation level of CREB was estimated by immunoblot analysis using specific antibodies. *B*, after the treatment with thapsigargin (5 μM) or BAPTA-AM (10 μM) for 2 h, the intracellular localization of phosphorylated CREB was examined by indirect immunofluorescence (*IF*) microscopy using specific antibodies as described under "Materials and Methods." The data represent two independent experiments.

gin, but decreased with BAPTA-AM, indicating that the phosphorylation status is regulated by the change of $[Ca^{2+}]_i$. In Fig. 9*B*, the intracellular localization of phosphorylated CREB (Ser-133) was investigated by indirect immunofluorescence microscopy in cells treated with or without the Ca^{2+} modulators. The fluorescent signals for phosphorylated CREB increased especially in the nucleus of the cells treated with thapsigargin, but it was significantly decreased by BAPTA-AM compared with untreated cells. These results are consistent with the results that the gene of *PP2Acα* is regulated via CRE in a Ca^{2+}-dependent manner.

DISCUSSION

Akt is a Ser/Thr protein kinase with antiapoptotic and oncogenic activities (8–10). With regard to the Ca^{2+}-dependent regulation of Akt, Conus *et al.* (15) reported that the activation of Akt was independent of Ca^{2+} in mouse fibroblasts treated with thapsigargin. However, Yano *et al.* (13) identified a Ca^{2+}-triggered signaling cascade in which CaMK kinase activates Akt in a PI 3-kinase-independent manner. Then Huber *et al.* (14) found that Akt was rapidly activated by treatment with thapsigargin through the activation of PI 3-kinase. In the present study, we found that Akt was suppressed by a long term elevation of $[Ca^{2+}]_i$ induced by thapsigargin, but was enhanced by a long term lowering of $[Ca^{2+}]_i$ caused by BAPTA-AM in H9c2 cells. The inactivation of Akt is highly correlated with susceptibility to apoptosis. Recently, Luo *et al.* (34) reported that inactivation of Akt is a causal mediator of cell death, and this is consistent with our present results. Although the underlying mechanism for these differences in the Ca^{2+}-dependent regulation of Akt was not clear, we showed that transcriptional regulation of PP2Acα was important to control the activation status of Akt in H9c2 cells under conditions where there is a long term change in $[Ca^{2+}]_i$ levels.

PP2A is a multifunctional protein Ser/Thr phosphatase that regulates a variety of signaling pathways in eukaryotic cells (35, 36, 37). The core structure is a dimer, consisting of a 36-kDa catalytic subunit (PP2Acα, β) and a 65-kDa constant regulatory (structural) subunit (PR65/Aα, β). A third, variable regulatory subunit (B, PR55/Bα, β, γ, δ; B′, PR56/61α, β, γ, δ, ε; B″, PR48/58/72/130; B‴, PR99/110) can associate with this core enzyme. There are various reports of PP2A as a positive regulator of apoptosis (38), although a specific subunit of PP2A containing B′/PR61 is reported to be inhibitory for apoptosis in *Drosophila* (39, 40). Bad is a pro-apoptotic member of the Bcl-2 family, whose function is highly regulated by reversible phosphorylation (41). PP2A was responsible for the dephosphorylation of Bad (42), and dephosphorylated Bad bound antiapoptotic Bcl-2 members at the mitochondrial membrane leading to apoptotic cell death (43). PP2A was also found to co-localize at the mitochondrial membrane with Bcl-2, and the proapoptotic sphingolipid ceramide has been shown to activate the PP2A involved (44, 45). In anti-Fas-induced apoptosis, activation of caspase-3 caused cleavage of the regulatory Aα subunit of PP2A, and this in turn increased PP2A activity (46). On the other hand, Liu *et al.* (47) reported that 4-hydroxynonenal induced dephosphorylation of Akt through activation of PP2A in a caspase-dependent apoptosis of Jurkat cells. In the study, the authors described that PP2A was activated by an altered intracellular localization of tyrosine-dephosphorylated PP2A, but not by the caspase-dependent cleavage of the regulatory Aα subunit of PP2A. Furthermore, C2-ceramide induced dephosphorylation of both GSK3β and Akt by activating PP2A, resulting in apoptosis in rat cerebellar granule cells, and the apoptosis was blocked with lithium by inhibiting PP2A activity (48). Together, these findings indicate that PP2A plays a critical role in the positive regulation of apoptosis by dephosphorylating various apoptotic regulators including Akt, but the molecular mechanism for the activation of PP2A in apoptosis is not clearly understood.

PP2A is considered a phosphatase responsible for the dephosphorylation and inactivation of Akt (47, 48, 49, 50, 51, 52, 53). Previously, we also showed that Akt was dephosphorylated by PP2A in H9c2 cells (16), and PP2A interacted transiently with Akt in H9c2 cells under oxidative stress with H_2O_2 (27). In the present study, the treatment with okadaic acid decreased PP2A activity to ~70% of the untreated control value, and it reversed the thapsigargin-dependent suppression of the phosphorylation of Akt in H9c2 cells (Fig. 4). Furthermore, treatment with okadaic acid could suppress the thapsigargin-induced enhancement of apoptosis in cells exposed to H_2O_2, although the effective okadaic acid concentration was limited to a range around 100–200 nM (Fig. 5). These findings strongly suggest that PP2A plays an up-regulating role in the thapsigargin-induced enhancement of apoptosis by inhibiting Akt signaling. Collectively, the finding that up-regulation of *PP2Acα* gene expression led to an increase of PP2A activity is consistent with the enhanced dephosphorylation and inactivation of Akt in H9c2 cells following the long term elevation of $[Ca^{2+}]_i$ due to thapsigargin exposure (Fig. 2). Although the expression of PP2Ac is tightly controlled by an autoregulatory translational mechanism (54), there are reports describing changes in PP2Ac levels, for instance, during all-*trans* retinoic acid-induced differentiation of HL-60 cells (55, 56), during adipocyte differentiation induced by peroxisome proliferator-activated receptor-γ (57), during stimulation by colony-stimulating factor in macrophages (58), and during a response to the disruption of cellular attachment in mouse C3 10T1/2 cells (59).

We also observed transcriptional activation of PP2Acα in H9c2 cells transfected with the expression vector for calreticulin, a molecular chaperone in the endoplasmic reticulum (16). However, the underlying mechanism for these differences in the regulation of PP2A expression was not clarified.

To investigate the molecular mechanism behind the Ca^{2+}-dependent transcriptional regulation of PP2Ac expression in H9c2 cells, the promoter function of the *PP2Acα* gene was characterized using a luciferase-based reporter assay in cells treated with Ca^{2+} modulators such as thapsigargin and BAPTA-AM. The results showed that the expression of PP2Acα was transcriptionally regulated by the change of $[Ca^{2+}]_i$. The *PP2Ac* gene has been isolated and characterized in humans (60) and rats (23). In both species, the promoter region of PP2Acα has a high GC content and does not contain either a TATA box or a CAAT box, which suggests that the gene is a typical housekeeping gene. Among various transcription factors including CREB, Sp1, and RORα within the promoter region, CREB was revealed to be responsible for Ca^{2+}-dependent regulation of the *PP2Acα* gene in H9c2 cells treated with thapsigargin and BAPTA-AM. CREB is a bZIP transcription factor that forms homo- or heterodimers with itself or other members of the CREB family including ATF1 and CREM, and is a pivotal transcription factor that regulates cell proliferation, differentiation, and survival in a variety of cell types in vertebrates (33). The CREB dimers interact with a specific DNA sequence having the consensus motif TGACGTCA in the regulatory region of CREB target genes. CREB is inactive as a transcription factor until a cell is exposed to any extracellular stimuli that trigger its phosphorylation at a specific site, Ser-133, within its kinase-inducible domain (33). CREB was originally identified as a target of the cAMP signaling pathway, and regulated in response to diverse signals, including peptide hormones, growth factors, and Ca^{2+}. CREB is known to be activated at high $[Ca^{2+}]_i$ and this is consistent with our findings that the level of CREB phosphorylated at Ser-133 increased with thapsigargin but decreased with BAPTA-AM in the nucleus of H9c2 cells. Though minute changes in $[Ca^{2+}]_i$ are quickly transformed into changes in the activity of several kinases including cAMP-dependent kinase, protein kinase C, MAPKs, Ca^{2+}/CaMK and CaMK kinase, it is not clear whether these kinases are influenced in the case of long term change of $[Ca^{2+}]_i$ in H9c2 cells treated with Ca^{2+} modulators. Among these kinases, CaMKII and CaMKIV were reported to be able to phosphorylate CREB directly (61, 62). In addition, Rsk protein kinase phosphorylates CREB at Ser-133 through activation of the Ras/MAPK signaling pathway by Ca^{2+} (63, 64). Although CaMKIV mediates the early phase in the phosphorylation of Ser-133 in membrane-depolarized neurons, the MAPK pathway is responsible for prolonging the phosphorylation (65). In the present study, an increase in both the phosphorylation of CREB at Ser-133 and activity of CREB to bind the CRE site was observed after 2 h treatment with thapsigargin, suggesting a late activation of CREB caused by the long term elevation of $[Ca^{2+}]_i$. The treatment with BAPTA-AM influenced the phosphorylation of CREB and suppressed the binding of CREB to the CRE after 1 h, and this also suggests a late inactivation of CREB on the long term suppression of $[Ca^{2+}]_i$. Taken together, the long term change of $[Ca^{2+}]_i$ may regulate CREB function through the MAPK pathway rather than CaMK pathway in H9c2 cells treated with Ca^{2+} modulators.

Thapsigargin causes an increase of $[Ca^{2+}]_i$, and is also known as an inducer of endoplasmic reticulum (ER) stress (unfolding protein stress in the ER) (66). Recently, Song *et al.* (67) reported that thapsigargin-induced ER stress induced dephosphorylation of both GSK3β and Akt by activating PP2A, resulting in apoptosis in neuroblastoma cells, and this was consistent with our results. In the study, the authors described that dephosphorylation of GSK3β by activated PP2A was critical for the activation of caspase-3 in ER stress-induced apoptosis, but the mechanism for the PP2A activation by ER stress was not clarified. In ER stress, a transcriptional up-regulation is seen in the ER stress responsive genes that code a variety of ER proteins related to molecular chaperone functions, such as BiP/Grp78, Grp94, Grp58/ERp57, ERp72, and calreticulin (66). In mammalian cells, the 19-nucleotide motif CCAAT-N9-CCACG was identified as an ER responsive element (ERSE) of various ER chaperone genes, and was recognized by the human bZIP transcriptional factor ATF6 for ER stress response (68). However, we could not find a consensus sequence within the 1.6-kbp promoter region of the *PP2Acα* gene, and this suggests that the *PP2Acα* gene is not a direct target for the ER stress response in thapsigargin-treated cells.

In this study, CREB was linked to the enhanced susceptibility to apoptosis through the induction of the *PP2Ac* gene in cells exposed to the long term elevation of $[Ca^{2+}]_i$. To further investigate whether CREB is specifically responsible for the up-regulation of apoptosis in cells treated with thapsigargin and H_2O_2, CREB expression was suppressed by the short interfering RNA (siRNA) for the CREB gene. Using mammalian CREB siRNA expression plasmid (pKD-CREB-v2, Upstate Biotechnology), the CREB expression level was suppressed in H9c2 cells to ~30% of non-transfected cells. Using the transfected cells, thapsigargin-dependent enhancement of cell damage and apoptosis were examined in cells treated with thapsigargin (5 μM) and H_2O_2 (75 μM). However, despite the suppression of CREB protein, cell damage and apoptosis were not inhibited in cells treated with thapsigargin and H_2O_2, but rather were more enhanced (data not shown). This indicates that CREB is not specifically responsible for the mechanism enhancing apoptosis in cells showing long term elevation of $[Ca^{2+}]_i$. However, this may be reasonable because CREB is well known as a transcription factor for cell survival and antiapoptotic genes such as Bcl-2 (69), and the suppression of CREB may firstly decrease the expression of such cell survival genes resulting in enhanced susceptibility to apoptosis. The effect of the suppressed expression of CREB on cell survival was also consistent with previous findings using dominant-negative CREB polypeptides (69). Although the suppressed expression of CREB itself did not specifically reduce the thapsigargin-dependent enhancement of apoptotic cell damage in H9c2 cells, it still may be possible that CREB works for apoptosis on some negative feedback-like loop of cell survival signaling in cells demonstrating long term elevation of $[Ca^{2+}]_i$.

In conclusion, we found that the Akt kinase pathway was regulated by a long term change of $[Ca^{2+}]_i$ through transcriptional regulation of PP2Acα. With an elevation of $[Ca^{2+}]_i$ induced by thapsigargin, *PP2Acα* gene expression is up-regulated through the activation of CRE at a late phase of the response. As a consequence, Akt is dephosphorylated and inactivated by PP2A, and this leads to an increase in susceptibility to apoptosis under the conditions with thapsigargin. Although the activation of CRE has been considered to function as a cell survival signaling, Ca^{2+}-induced late activation of CRE leads to an enhancement of apoptotic signaling, and this suggests some feedback mechanism of CRE-mediating cell survival signaling. Luo *et al.* (34) reported that NMDA-induced deactivation of Akt was causative of neural cell death, and this suggests some Ca^{2+}-dependent mechanism is involved in the inactivation of Akt. Although the Ca^{2+}-dependent regulation of cell survival and death has been extensively studied (1, 3, 4), the

present findings may indicate another novel regulatory pathway of Akt through PP2A in the cell survival signaling controlled by calcium homeostasis.

Acknowledgments—We thank Drs. Kunimi Kikuchi and Hiroshi Shima for generously providing the rat PP1cc and PP2Acα cDNAs, and useful suggestions. We also thank Midori Ikezaki and Akiko Emura for technical assistance.

REFERENCES

1. Berridge, M. J., Lipp, P., and Bootman, M. D. (2000) *Nat. Rev.* **1**, 11–21
2. Agell, N., Bachs, O., Rocamora, N., and Villalonga, P. (2002) *Cell. Signal.* **14**, 649–654
3. Orrenius, S., Zhivotovsky, B., and Nicotera, P. (2003) *Nat. Rev.* **5**, 552–565
4. Rizzuto, R., Pinton, P., Ferrari, D., Chami, M., Szabadkai, G., Magalhaes, P. J., Virgilio, F., and Pozzan, T. (2003) *Oncogene* **22**, 8619–8627
5. Murrell, C. L., and Mochly-Rosen, D. (2003) *Arch. Biochem. Biophys.* **420**, 246–254
6. Crabtree, G. R. (2001) *J. Biol. Chem.*, **276**, 2313–2316
7. Klumpp, S., and Krieglstein, J. (2002) *Curr. Opin. Pharmacol.* **2**, 458–462
8. Brazil, D. P., and Hemmings, B. A. (2001) *Trends Biochem. Sci.*, **26**, 657–664
9. Scheid, M. P., and Woodgett, J. R. (2003) *FEBS Lett.* **546**, 108–112
10. Franke, T. F., Hornik, C. P., Segev, L., Shostak, G. A., and Sugimoto, C. (2003) *Oncogene* **22**, 8983–8998
11. Ozes, O. N., Mayo, L. D., Gustin, J. A., Pfeffer, S. R., Pfeffer, L. M., and Donner, D. B. (1999) *Nature* **401**, 82–85
12. Romashkova, J. A., and Makarov, S. S. (1999) *Nature*, **401**, 86–90
13. Yano, S., Tokumitsu, H., and Soderling, T. R. (1998) *Nature* **396**, 584–587
14. Huber, M., Hughes, M. R., and Krystal, G. (2000) *J. Immunol.* **165**, 124–133
15. Conus, N. M., Hemmings, B. A., and Pearson, R. B. (1998) *J. Biol. Chem.* **273**, 4776–4782
16. Kageyama, K., Ihara, Y., Goto, S., Urata, Y., Toda, G., Yano, K., and Kondo, T. (2002) *J. Biol. Chem.* **277**, 19255–19264
17. Hescheler, J., Meyer, R., Plant, S., Krautwurst, D., Rosenthal, W., and Schultz, G. (1991) *Circ. Res.* **69**, 1476–1486
18. Grynkiewcz, G., Poenie, M., and Tsien, R. Y. (1985) *J. Biol. Chem.* **260**, 3440–3450
19. Gevrieli, Y., Sherman, Y., and Benn-Sasson, S. A. (1992) *J. Cell Biol.* **119**, 493–501
20. Kitamura, K., Mizuno, Y., Sasaki, A., Yazui, A., Tsuiki, S., and Kikuchi, K. (1991) *J. Biochem.* **109**, 307–310
21. Kitagawa, Y., Takita, T., Ikeda, I., Kikuchi, K., Tsuiki, S., Sugimura, T., and Nagao, M. (1988) *Biochim. Biophys. Acta.* **961**, 123–129
22. Ihara, Y., Sakamoto, Y., Mihara, M., Shimizu, K., and Taniguchi, N. (1997) *J. Biol. Chem.* **272**, 9629–9634
23. Kitagawa, Y., Shima, H., Sasaki, K., and Nagao, M. (1991) *Biochim. Biophys. Acta.* **1060**, 339–344
24. Muroya T., Ihara Y., Ikeda S., Yasuoka C., Miyahara Y., Urata Y., Kondo T., and Kohno S. (2003) *Biochem. Biophys. Res. Commun.* **300**, 905–910
25. Thastrup, O., Cullen, P. J., Drobak, B. K., Hanley, M. R., and Dawson, A. P. (1990) *Proc. Natl. Acad. Sci., U. S. A.* **87**, 2466–2470
26. Pan, Z., Bhat, M. B., Niaminen, A.-L., and Ma, J. (2001) *J. Biol. Chem.* **276**, 32257–32263
27. Murata, H., Ihara, Y., Nakamura, H., Yodoi, J., Sumikawa, K., and Kondo, T. (2003) *J. Biol. Chem.* **278**, 50226–50233
28. Dolmetsch, R. E., Lewis, R. S., Goodnow, C. C., and Healy, J. I. (1997) *Nature* **386**, 855–858
29. Haystead, T. A. J., Sim, A. T. R., Carling, D., Honnor, R. C., Tsukitani, Y., Cohen, P., and Hardie, D. G. (1989) *Nature* **337**, 78–81
30. Gehringer, M. M. (2004) *FEBS Lett.* **557**, 1–8
31. Bouwman, P., and Philipsen, S. (2002) *Mol. Cell. Endocrinol.* **195**, 27–38
32. Kane, C. D., and Means, A. R. (2000) *EMBO J.* **19**, 691–701
33. Shaywitz, A. J., and Greenberg, M. E. (1999) *Annu. Rev. Biochem.* **68**, 821–861
34. Lee, H. R., Hattori, H., Hossain, M. A., Hester, L., Huang, Y., Lee-Kwon, W., Donowitz, M., Nagata, E., and Snyder, S. H. (2003) *Proc. Natl. Acad. Sci., U. S. A.* **100**, 11712–11717
35. Milward, T. A., Zolnierowicz, S., and Hemmings, B. A. (1999) *Trends Biochem. Sci.* **24**, 186–191
36. Sontag, E. (2001) *Cell. Signal.* **13**, 7–16
37. Janssens, V., and Goris, J. (2000) *Biochem. J.* **353**, 417–439
38. Van Hoof, C., and Goris, J. (2003) *Biochim. Biophys. Acta* **1640**, 97–104
39. Silverstein, A. M., Barrow, C. A., Davis A. J., and Mumby M. C. (2002) *Proc. Natl. Acad. Sci., U. S. A.* **99**, 4221–4226
40. Li, X., Scuderi, A., Letsou, A., and Virshup, D. M. (2002) *Mol. Cell. Biol.* **22**, 3674–3684
41. Cory, S., Huang, D. C. S., and Adams, J. M. (2003) *Oncogene* **22**, 8590–8607
42. Chiang, C. W., Harris, G., Ellig, C., Masters, S. C., Subramanian, R., Shenolikar, S., Wadzinski, B. E., and Yang, E. (2001) *Blood* **97**, 1289–1297
43. Datta, S. R., Katsov, A., Hu, L., Petros, A., Fesik, S. W., Yaffe, M. B., and Greenberg, M. E. (2000) *Mol. Cell*, **6**, 41–51
44. Ruvolo, P. P., Deng, X., Ito, T., Carr, B. K., and May, W. S. (1999) *J. Biol. Chem.* **274**, 20296–20300
45. Ruvolo, P. P., Clark, W., Mumby, F., Gao, W. S., and May, W. S. (2002) *J. Biol. Chem.* **277**, 22847–22852
46. Santore, M. F., Anuand, R. R., Robertson, M. M., Peng, Y. W., Brady, M. J., Mankovich, J. A., Hackett, M. C., Ghayur, T., Walter, G. W., Wong, W. W., and Giegel, D. A. (1998) *J. Biol. Chem.* **273**, 13119–13128
47. Liu, W., Akhand, A. A., Takeda, K., Kawamoto, Y., Itoigawa, M., Kato, M., Suzuki, H., Ishikawa, N., and Nakashima, I. (2003) *Cell Death Differ.* **10**, 772–781
48. Mora, A., Sabio, G., Risco, A. M., Cuenda, A., Alonso J. C., Soler, G., and Centeno, F. (2002) *Cell. Signal.* **14**, 557–562
49. Andjelkovic, M., Jakubowics, T., Cron, P., Ming, X.-F., Han, J.-W., and Hemmings, B.A. (1996) *Proc. Nat. Acad. Sci., U. S. A.* **93**, 5699–5704
50. Meier, R., Thelen, M., and Hemmings, B. A. (1996) *EMBO J.* **17**, 7294–7303
51. Chen, D., Ficini, R. V., Olson, A. L., Hemmings, B. A., and Pessin, J. E. (1999) *Mol. Cell. Biol.* **19**, 4584–4694
52. Resjo, S., Goransson, O., Harndahl, L., Zolnierowicz, S., Manganiello, V., and Degerman, E. (2002) *Cell. Signal.* **14**, 231–238
53. Ivaska, J., Nissinen, L., Immonen, N., Eriksson, J. E., Kahari, V. M., and Heino, J. (2002) *Mol. Cell. Biol.* **22**, 1352–1359
54. Baharian, Z., and Schonthal, A. H. (1998) *J. Biol. Chem.* **273**, 19019–19024
55. Tawara, I., Nishikawa, M., Morita, K., Kobayashi, K., Toyoda, H., Omay, S. B., Shima, H., Nagao, M., Kuno, T., Tanaka, C., and Shirakawa, S. (1993) *FEBS Lett.* **321**, 224–228
56. Nishikawa, M., Omay, S. B., Toyoda, H., Tawara, I., Shima, H., Nagao, M., Hemmings, B. A., Mumby, M. C., and Deguchi, K. (1994) *Cancer Res.* **54**, 4879–4884
57. Altick, S., Xu, M., and Spiegelman, B. M. (1998) *Genes Dev.* **11**, 1987–1998
58. Wilson, N. J., Moss, S. T., Cear, X. P., Ward, A. C., and Hamilton, J. A. (1999) *Biochem. J.* **339**, 517–524
59. Campos, S. V., and Schonthal, A. H. (2000) *J. Cell. Physiol.* **183**, 88–96
60. Khew-Goodall, Y., Mayer, R. E., Maurer, F., Stone, S. R., and Hemmings, B. A. (1991) *Biochemistry* **30**, 89–97
61. Wu, X., and McMurray, C. T. (2001) *J. Biol. Chem.* **276**, 1735–1741
62. Kornhauser J. M., Cowan, C. W., Shaywitz, A. J., Dolmetsch, R. E., Griffith, E. C., Hu, L. S., Haddad, C., Xia, Z., and Greenberg, M. E. (2002) *Neuron* **34**, 221–233
63. Rosen, L., Ginty, D., Weber, M., and Greenberg, M. (1994) *Neuron* **12**, 1207–1221
64. Xing, J., Ginty, D. D., and Greenberg, M. E. (1996) *Science* **273**, 959–963
65. Wu, G.-Y., Deisseroth, K., and Tsien, R. W. (2001) *Proc. Natl. Acad. Sci., U. S. A.* **98**, 2808–2813
66. Kaufman, R. J. (1999) *Genes Dev.* **13**, 1211–1233
67. Song, L., De Sarno, P., and Jope, R. S. (2002) *J. Biol. Chem.* **277**, 44701–44708
68. Yoshida, H., Haze, K., Yanagai, H., Yura, T., and Mori, K. (1998) *J. Biol. Chem.* **273**, 33741–33749
69. Mayr, B., and Montminy, M. (2001) *Nat. Rev. Mol. Cell. Biol.* **2**, 599–609

Free Radical Biology & Medicine, Vol. 37, No. 11, pp. 1875–1884, 2004

0891-5849/$-see front matter

ELSEVIER

doi:10.1016/j.freeradbiomed.2004.09.002

Original Contribution

NUCLEAR GLUTATHIONE *S*-TRANSFERASE π PREVENTS APOPTOSIS BY REDUCING THE OXIDATIVE STRESS-INDUCED FORMATION OF EXOCYCLIC DNA PRODUCTS

KENSAKU KAMADA,*,[1] SHINJI GOTO,†,[1] TOMOHIRO OKUNAGA,* YOSHITO IHARA,† KENTARO TSUJI,‡ YOSHICHIKA KAWAI,‡,[2] KOJI UCHIDA,‡ TOSHIHIKO OSAWA,‡ TAKAYUKI MATSUO,* IZUMI NAGATA,* and TAKAHITO KONDO†

*Department of Neurosurgery and †Department of Biochemistry and Molecular Biology in Disease, Atomic Bomb Disease Institute, Nagasaki University Graduate School of Biomedical Sciences, Nagasaki 851-8523, Japan; and ‡Laboratory of Food and Biodynamics, Nagoya University Graduate School of Bioagricultural Sciences, Nagoya, Japan

(*Received* 7 *June* 2004; *Revised* 24 *August* 2004; *Accepted* 2 *September* 2004)
Available online 25 September 2004

Abstract—We previously found that nuclear glutathione *S*-transferase π (GSTπ) accumulates in cancer cells resistant to anticancer drugs, suggesting that it has a role in the acquisition of resistance to anticancer drugs. In the present study, the effect of oxidative stress on the nuclear translocation of GSTπ and its role in the protection of DNA from damage were investigated. In human colonic cancer HCT8 cells, the hydrogen peroxide (H_2O_2)-induced increase in nuclear condensation, the population of sub-G_1 peak, and the number of TUNEL-positive cells were observed in cells pretreated with edible mushroom lectin, an inhibitor of the nuclear transport of GSTπ. The DNA damage and the formation of lipid peroxide were dependent on the dose of H_2O_2 and the incubation time. Immunological analysis showed that H_2O_2 induced the nuclear accumulation of GSTπ but not of glutathione peroxidase. Formation of the 7-(2-oxo-hepyl)-substituted 1,N^2-etheno-2′-deoxyguanosine adduct by the reaction of 13-hydroperoxyoctadecadienoic acid (13-HPODE) with 2′-deoxyguanosine was inhibited by GSTπ in the presence of glutathione. The conjugation product of 4-oxo-2-nonenal, a lipid aldehyde of 13-HPODE, with GSH in the presence of GSTπ, was identified by LS/MS. These results suggested that nuclear GSTπ prevents H_2O_2-induced DNA damage by scavenging the formation of lipid-peroxide-modified DNA.

Keywords—Oxidative stress, DNA damage, Glutathione *S*-transferase π, 7-(2-Oxo-hepyl)-substituted 1,N^2-etheno-2′-deoxyguanosine adduct, Free radical

INTRODUCTION

The role of oxidative stress as a mediator of apoptosis has been extensively studied. In particular, hydrogen peroxide (H_2O_2), a by-product of oxidative stress and a major reactive oxygen species (ROS), has been implicated in triggering apoptosis in various cells. H_2O_2 induces peroxidation of cellular components such as proteins, lipids, and nucleic acids [1]. H_2O_2 also stimulates intracellular signal cascades, such as mitogen-activated protein kinases, and activates transcription factors, such as AP-1 and nuclear factor kappa-B [2].

Glutathione *S*-transferase (GST, EC 2.5.1.18) is mainly expressed in the cytoplasm and is ubiquitous in nature. GST functions in xenobiotic biotransformation [3], drug metabolism [4], protection against peroxidative stress of lipids and the nucleus [5–7], and isomeration of prostaglandins [8]. Human GSTπ is one of a family of

Address correspondence to: Takahito Kondo, Department of Biochemistry and Molecular Biology in Disease, Atomic Bomb Disease Institute, Nagasaki University Graduate School of Medicine, Nagasaki 851-8523, Japan; Fax: +81 (95) 849 7100; E-mail: kondo@net.nagasaki-u.ac.jp.

[1] Contributed equally to this work.

[2] Present address: Department of Food Science, Graduate School of Nutrition and Biosciences, University of Tokushima, Japan.

GSTs; it has been reported to accumulate in various human cancer tissues or precancer tissues and is employed in cancer research as a tumor marker [9–13]. An increase in GSTπ was also found in cancer cell lines resistant to doxorubicin hydrochloride (DOX), *cis*-diamminedichloroplatinum(II) (cisplatin: CDDP) [14–16], and alkylating agents [17].

In addition to its main location in the cytoplasm, GSTπ has been found in the nucleus in uterine cancer cells [18] and glioma cells [19]. These findings suggest a negative correlation between the existence of GSTπ in the nucleus of cancer cells and the survival of the patient. However, there has been no report on the mechanisms responsible for the nuclear survival of GSTπ or on the physiological role of nuclear GSTπ.

Edible mushroom lectin (*Agaricus bisporus* lectin; ABL) efficiently internalizes into the cytoplasm of cultured cells, localizes around the nucleus, and inhibits the nuclear transfer of proteins [20]. Previous reports presented evidence that ABL inhibits the nuclear transport of GSTπ and increases the sensitivity of cancer cells to anticancer drugs [21,22].

Endogenous lipid peroxidation products react with DNA and exocyclic DNA adducts to cause the covalent modification of nuclear bases [23,24]. During the lipid peroxidation process, lipid hydroperoxides are formed as the initial products, and the decomposition of the lipid hydroperoxides leads to the formation of aldehydes as the end products. Several aldehydes possess high reactivity against DNA bases, especially guanine [25–27]. Lipid-peroxide-induced DNA adduct formation and site-specific cleavage of double-stranded DNA have been reported [28,29]. Previously, Kawai et al. [30] studied the reaction of lipid hydroperoxides with DNA components and established a method to detect the formation of 7-(2 oxo-hepyl)-substituted 1,N^2-etheno-2′-deoxyguanosine adducts (oxo-heptyl-εdG) by the reaction of 13-hydroperoxyoctadecadienoic acid (13-HPODE) with 2′-deoxyguanosine (dG).

Recently, it was reported that 4-hydroxy-2-nonenal (4-HNE) and 4-oxo-2-nonenal (4-ONE), the end products of lipid peroxides, are nonenzymatically transformed to conjugate with GSH [31]. Moreover, 4-ONE, a major end product of 13-HPODE, had a higher affinity for the nucleus than 4-HNE. Even though it has been found that GSTs catalyzes the formation of a conjugate of 4-HNE with GSH [32], its role in the formation of 4-ONE-GSH adducts was not known. In this study, we examined whether the nuclear GSTπ plays a role in the cellular sensitivity to oxidative stress caused by H_2O_2 and found that GSTπ prevents DNA damage by scavenging the oxo-heptyl-εdG formed from 13-HPODE and forming a conjugate of 4-ONE with GSH.

MATERIALS AND METHODS

Materials

ABL was purchased from Wako Pure Chemical Industries Ltd. (Osaka, Japan). RPMI 1640 medium and fetal bovine serum (FBS) were obtained from Invitrogen Corp. (Carlsbad, CA). Sheep polyclonal antibodies against human glutathione peroxidase (GPX) were purchased from The Binding Site Ltd. (Birmingham, UK). Horseradish peroxidase (HRP)-labeled anti-rabbit IgG, HRP-labeled anti-mouse IgG, and HRP-labeled anti-sheep IgG were from DAKO A/S (Glostrup, Denmark). The Enhanced Chemiluminescence (ECL) kit was obtained from Amersham Biosciences (Buckinghamshire, UK). All other chemicals and reagents were purchased from Sigma Aldrich (St. Louis, MO).

Preparation of cells

We used the human cancer cell lines HCT8 (colonic carcinoma) kindly donated by Dr. K. J. Scanlon. HCT8 cells were supplemented with 10% FBS at 37°C in 5% CO2 with 100% humidity. Six hours before treatment with ABL, the cells were maintained in medium with 1% FBS. About 2×10^6 cells were harvested with trypsin and washed with phosphate-buffered saline (0.137 M NaCl, 2.68 mM KCl, and 10 mM NAH2PO4/Na2HPO4, pH 7.4: PBS) twice at 4°C. The pellets were stored at −80°C before use.

TUNEL assay

The terminal deoxynucleotidyl transferase-mediated dUTP nick end labeling (TUNEL) assay was performed using an Apop Tag Plus Fluorescein in situ Apoptosis Detection Kit (Intergen Co., Purchase, NY). Briefly, approximately 2×10^6 cells were harvested, fixed in 70% ethanol, treated with terminal deoxynucleotidyl transferase for 1 h and then flourescein isothiocyanate (FITC) conjugate anti-digoxigenin for 1 h at room temperature, washed with 0.1% Triton X-100/PBS, and resuspended in propidium iodide containing RNase A. Fluorescence intensity was estimated simultaneously using a FACScan flow cytometer (Becton–Dickinson, San Jose, CA).

Nuclear condensation

For the histochemical analysis, HCT8 cells were maintained with RPMI 1640 medium containing 10% FBS in a four-well Lab Tec Chamber (Nalge Nunc International, Naperville, IL). After treatment with H_2O_2, cells were treated with 10 μM Hoechst 33342 for 30 min to estimate the extent of nuclear condensation. They were then washed again with PBS. Fluorescence intensity was examined using an Axioskop2 fluorescence microscope (Carl Zeiss, Jena, Germany), and the findings were

analyzed using a charge-coupled device camera (Axio-Cam) and AxioVison software.

Analysis of double-stranded breaks of DNA

DNA damage was determined by flow cytometry, based on the formation of sub-G1 peaks of DNA as described by Gong et al. [33]. HCT8 cells were washed with PBS, fixed with 70% ethanol for 12 h at -20°C, and then centrifuged and further incubated with citrate–phosphate buffer (1 v of 0.1 M citric acid and 24 v of 0.2 M Na_2HPO_4) for 15 min at 25°C. The DNA content per nucleus was evaluated in a FACScan flow cytometer after the nuclei were stained with propidium iodide.

Preparation of proteins

The cytoplasmic and nuclear proteins were prepared as described by Digram et al. [34]. Proteins in the whole cells were prepared as described previously [35].

Preparation of antibodies

GSTπ was purified from human placenta, and polyclonal antibody against human GSTπ was obtained by immunizing rabbits as described previously [21]. The monoclonal antibody to Oxo-heptyl-edG was prepared as described previously [30].

Immunological estimation

Immunological levels of GSTπ in the cytoplasm and nucleus were estimated by Western blotting. Lysate from the extract of cells was separated by SDS–polyacrylamide gel electrophoresis (SDS–PAGE) in a 12.5% gel, transferred to a nitrocellulose membrane, and immunologically stained using rabbit IgG against human GSTπ or sheep IgG against human GPX as the primary antibody and HRP-labeled anti-rabbit IgG or HRP-labeled anti-sheep IgG as the secondary antibody. Blots were developed by enhanced chemiluminescence using the ECL kit and the relative immunological activity was analyzed by NIH Image. The protein concentration was determined according to Redinbaugh and Turley [36], with bovine serum albumin as the standard.

Estimation of lipid peroxide in the nucleus

Nuclei extracts were prepared as described by Abmayr and Warkman [37]. Nuclear thiobarbituric acid reactive substance (TBARS) levels were determined according to the method of Ohkawa et al. [38] using tetramethoxyprepane (Wako Pure Chemical Industries).

Estimation of oxo-heptyl-edG

Cells incubated in various conditions were harvested with trypsin and washed with PBS two times at 4°C. The cells were then suspended in 10 mM citrate buffer (pH 6.0) and incubated for 10 min at 95°C. After a wash with PBS two times, the cells were suspended in 2 M HCl for 30 min at room temperature and rewashed with PBS two times. The levels of oxo-heptyl-εdG in the cells were estimated by flow cytometry using anti-oxo-heptyl-εdG mouse monoclonal antibody (mAb6A3) and FITC-conjugated anti-mouse IgG antibody.

Effect of GSTπ on the formation of oxo-heptyl-edG

13-HPODE (20 mM) was mixed with 1 mM $FeCl_2$ and stood for 12 h at 37°C. The solution (13-HPODE, 5 mM and $FeCl_2$, 0.2 mM, as a final concentration) was incubated with or without GSH (1 or 5 mM) and GSTπ (0.2 U) in the presence of 5 μg of calf thymus DNA for 1 h at 37°C. Then 1 and 5 μg of DNA extracted from the solution by ethanol precipitation

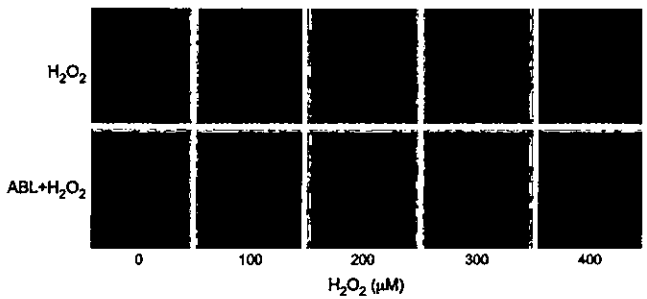

Fig. 1. Nuclear condensation. For the estimation of nuclear condensation, cells were incubated in a four-well Lab Tec Chamber. After treatment with various concentrations of H_2O_2 for 24 h, cells were treated with 10 μM Hoechst 33342 for 30 min for the estimation of nuclear condensation (top). The observation of fluorescence intensity was done using an Axioskop fluorescence microscope, and the findings were analyzed using a charge-coupled device camera and Axio Vision software. Cells were pretreated with ABL (40 μg/ml) for 10 h and then treated with H_2O_2 (bottom).

were spotted on a nitrocellulose membrane and immunologically stained using MAb6A3 as the primary antibody and HRP-conjugated anti-mouse IgG antibody as the secondary antibody. Blots were developed by enhanced chemiluminescence using the ECL kit and the relative immunological activity was analyzed by NIH Image.

Liquid chromatography/mass spectrometry

The chemical structure of the product of the incubation of 4-ONE and GSH in the presence of GSTπ was characterized by liquid chromatography/mass spectrometry (LC/MS). The LC/MS was conducted using a Platform II (VG Biotech) in an electrospray ionization positive (ESP+) mode. The gradient condition (solvent A, 0.01% trifluoroacetate; solvent B, acetonitrile containing 0.01% trifluoroacetate) was as follows: 100% A (0 min), 50% B (20 min), 100% B (30 min), 100% B hold (30–35 min), 100% A (40 min).

Statistical analysis

Data are presented as the mean ± SD. Differences were examined using a Student *t* test. A value of $p < 0.05$ was considered significant.

RESULTS

Nuclear condensation

Nuclear condensation is a characteristic of apoptosis. The nuclear condensation caused by H_2O_2 was estimated morphologically using Hoechst 33342 (Fig. 1). Human colonic cancer HCT8 cells were incubated with various concentrations of H_2O_2 for 24 h. No DNA condensation was observed (100–400 μM H_2O_2). ABL, a mushroom lectin, inhibits the nuclear transfer of GSTπ [1]. The cells were previously treated with 40 μg/ml of ABL for 10 h and further incubated with H_2O_2 for 24 h. Nuclear condensation was observed in

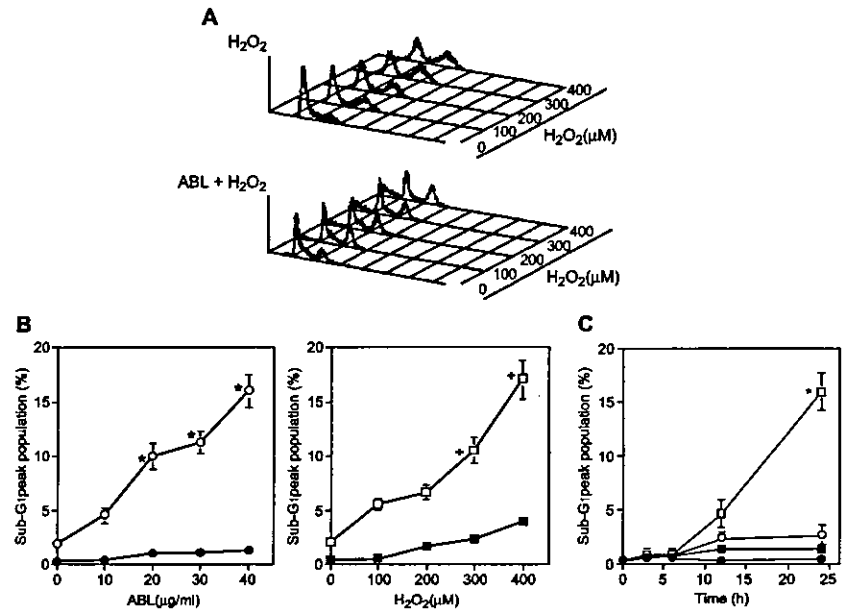

Fig. 2. Flow cytometric analysis of the DNA damage. (A) Effect of H_2O_2 on the DNA damage was analyzed using a FACScan flow cytometer. The sub-G_1 peak was estimated as a marker of the double-strand break of DNA. Treatment of cells with H_2O_2 or pretreatment with ABL was performed as described in Fig. 1 legend. (B) Effect of various concentrations of ABL (left) and H_2O_2 (right) on the formation of the sub-G_1 peak (%). ○400 μM H_2O_2 (+); ●H_2O_2 (−); □40 μg/ml ABL (+); ■ABL (−). *$p < 0.05$ compared with cells without H_2O_2 treatment. *$p < 0.05$ compared with cells without ABL pretreatment. (C) Effect of incubation time on the formation of the sub-G_1 peak (%). ○400 μM H_2O_2 (+); ●control; □40 μg/ml ABL (+); □400 μM H_2O_2 with ABL pretreatment. *$p < 0.05$ compared with H_2O_2-treated cells. Data are the means of three independent analyses. Bars show the SD.

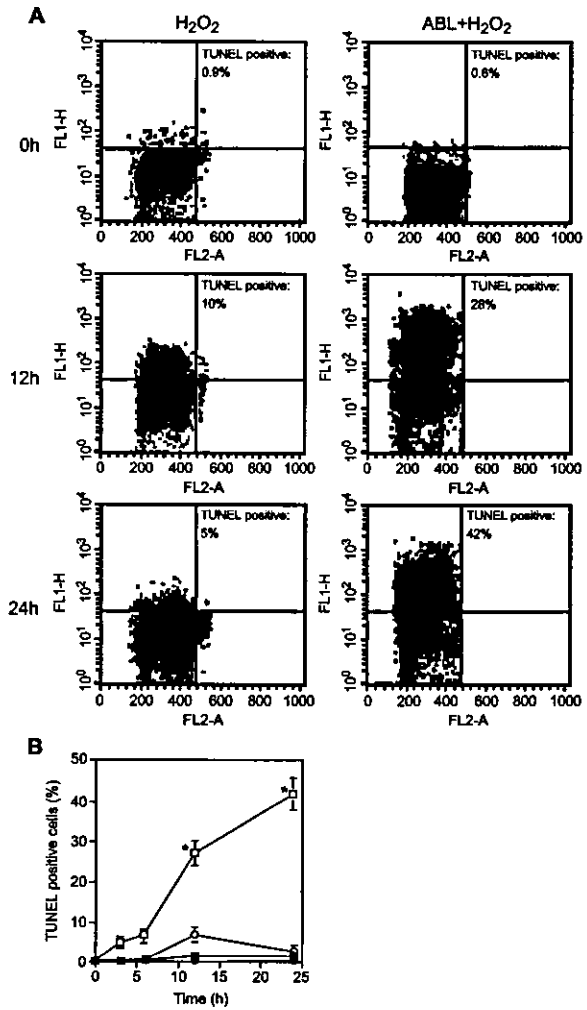

Fig. 3. TUNEL assay. The effect of ABL on the cytotoxicity of H_2O_2 was examined by TUNEL assay using an Apop Tag Plus Fluorescein In Situ Apoptosis Detection Kit as described under Materials and methods. (A) Cells (2×10^6) treated with 400 μM H_2O_2 for 12 and 24 h (left) or pretreated with ABL (40 μg/ml) for 10 h (right). (B) Effect of incubation time on the TUNEL-positive cells (%). ○400 μM H_2O_2 (+); ●control; □40 μg/ml ABL (+); ■400 μM H_2O_2 with ABL pretreatment. Data are the means of three independent analyses. Bars show the SD. *$p < 0.05$ compared with H_2O_2-treated cells.

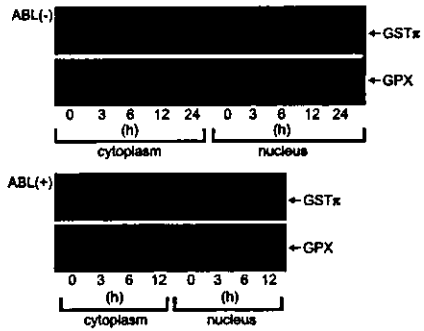

Fig. 4. Immunological estimation of the amount of GSTπ in the cytoplasm and nucleus. Proteins prepared from cellular cytoplasm and nucleus (1×10^5 cells) were separated by SDS–PAGE in a 12.5% gel, transferred to a nitrocellulose membrane, and immmunologically stained using rabbit IgG or sheep IgG antibody against human GSTπ or GPX. Cells were treated with 400 μM H_2O_2 for the period indicated with (bottom) or without (top) pretreatment with ABL for 10 h.

a manner dependent on the dose of H_2O_2 when the cells were pretreated with ABL. These results suggest that inhibition of the nuclear transfer of GSTπ by ABL enhanced the H_2O_2-induced DNA damage.

Effect of H_2O_2 on DNA damage

To understand the extent of the DNA damage by H_2O_2, the sub-G_1 peak was estimated flow cytometrically as a marker of the double-stranded breaks of DNA (Fig. 2A). The DNA damage induced by pretreatment with ABL was not apparent (Fig. 2B, left) and damage was slightly induced by H_2O_2 alone (Fig. 2B, right). ABL increased the population of the sub-G_1 peak induced by 400 μM H_2O_2 in a dose-dependent (10–40 μg/ml) manner (Fig. 2B, left). Pretreatment with 40 μg/ml of ABL for 10 h enhanced the population of the sub-G_1 peak induced by H_2O_2 (100–400 μM) for 24 h dose dependently (Fig. 2B, right). The effect of ABL on the H_2O_2-induced DNA damage was dependent on the incubation time with H_2O_2 (Fig. 2C). These results suggest that ABL increases the sensitivity of cells to H_2O_2.

TUNEL assay

The H_2O_2-induced DNA damage was also estimated by TUNEL assay (Fig. 3). At 400 μM H_2O_2 increased the proportion of TUNEL-positive cells in 12 h (10%) with a subsequent decrease at 24 h (5%). Pretreatment with ABL (40 μg/ml) caused an increase in TUNEL-positive cells induced by 400 μM H_2O_2, 28% in 12 h and 42% in 24 h (Figs. 3A and 3B). These results also suggest that ABL increases the sensitivity of cells to H_2O_2, leading to DNA damage and apoptosis.

Immunological estimation of nuclear GSTπ

The amount of GSTπ induced by H_2O_2 was estimated. Fig. 4 shows results of Western blotting for GSTπ. H_2O_2 increased the levels of cytoplasmic GSTπ in a time-dependent manner (top). A concomitant increase in the level of GSTπ was observed in the nucleus. The effect of ABL on the nuclear transfer of GSTπ was studied (bottom). The H_2O_2-induced transfer of GSTπ to the nucleus was inhibited by ABL. The results were consistent with previous data [21].

In the cytoplasm, H_2O_2 is detoxified to H_2O by GPX. Then, the immunological activity of GPX was estimated (Fig. 4). Treatment with H_2O_2 increased the levels of GPX in the cytoplasm. During the experiment, no GPX was transferred to the nucleus. Similarly, the immunological activity of glutathione reductase was not found in the nucleus in the presence or absence of H_2O_2 (data not shown).

Estimation of lipid peroxide in the nucleus

The formation of lipid peroxides was determined as the TBARS levels (Fig. 5). H_2O_2 increased the levels of nuclear TBARS when the cells were pretreated with ABL.

Role of nuclear GSTπ

Kawai et al. [30] reported that DNA bases are modified with lipid peroxide of linoleic acids leading to DNA damage. 4-ONE is nonenzymatically formed from 13-HPODE, which reacts with dG to form oxo-heptyl-edG. Doorn and Petersen [31] reported that 4-ONE has a higher affinity for nucleotides than 4-HNE and, on the other hand, spontaneously reacts with GSH to form its GSH conjugate [31]. We then speculated that

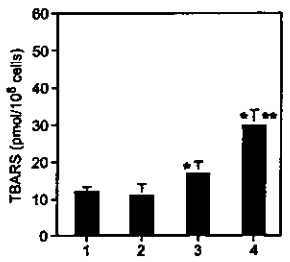

Fig. 5. Estimation of lipid peroxide in the nucleus. The formation of the nuclear TBARS was determined using tetramethoxyprepane. Data are the means of three independent analyses. Bars show the SD. *$p < 0.05$ compared with control cells. **$p < 0.05$ compared with H_2O_2-treated cells.

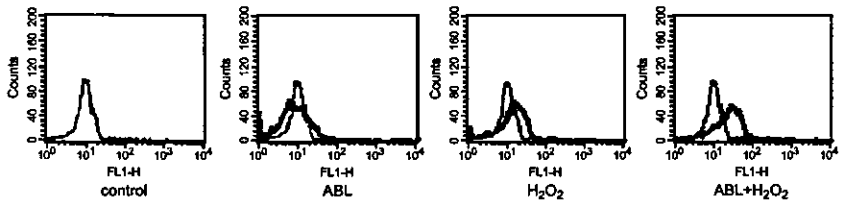

Fig. 6. Immunological estimation of oxo-heptyl-εdG. Effects of ABL (panel 2), H_2O_2 (panel 3), and H_2O_2 with ABL pretreatment (panel 4) on the levels of oxo-heptyl-εdG in the cells were estimated by flow cytometer using anti-oxo-heptyl-εdG mouse monoclonal antibody (mAb6A3) and FITC-conjugated anti-mouse IgG antibody.

human GSTπ catalyzed the formation of 4-ONE conjugated with GSH, which can then prevent the DNA from being modified with lipid peroxide. The immunological activity of lipid-peroxide-modified DNA was estimated flow cytometrically using anti-oxo-heptyl-εdG. The formation of oxo-heptyl-εdG was observed following treatment with 400 μM H_2O_2 for 12 h (Fig. 6, panel 3) and increased on pretreatment with ABL (Fig. 6, panel 4). The possible role of GSTπ in preventing the formation of lipid peroxide-DNA was affirmed in vitro. A mixture of 13-HPODE and $FeCl_2$ stood for 12 h at 37°C. The mixture was incubated with calf thymus DNA for 1 h at 37°C in the presence or absence of 5 mM GSH and 0.2 U of GSTπ. The formation of oxo-heptyl-εdG was estimated from immuno blots (Fig. 7). The formation of oxo-heptyl-εdG was inhibited by 20% in the presence of GSH (Fig. 7, lane 2) and by 60% in the presence of GSTπ and GSH (Fig. 7, lane 4). The results suggest that GSTπ inhibits the formation of oxo-heptyl-εdG in the nucleus. Fig. 8 shows the results of LC/MS measurements of the adduct formation of 4-ONE and GSH in the presence or absence of GSTπ. In the absence of GSTπ, the LC/MS analysis of the product gave a pseudomolecular ion peak [M + H]+ at *m/z* 462 (Fig. 8B). In the presence of GSTπ, this value apparently increased (Fig. 8C). Since the possible molecular weight of the ONE-GSH adduct is 641.18 (Fig. 9), the data obtained by LC/MS support the idea that GSTπ catalyzes the formation of the product.

DISCUSSION

In this study, we found for the first time that nuclear GSTπ functions to scavenge lipid-peroxide-induced DNA damage. We showed that (1) hydrogen peroxide increased the modification of nuclear DNA induced by lipid peroxide to cause DNA damage followed by the induction of apoptosis, (2) the nuclear GSTπ prevented DNA damage from lipid peroxide by scavenging the oxo-heptyl-εdG formed by the reaction of 13-HPODE with dG (the product of the conjugation of 4-ONE, one of the major breakdown products of 13-HPODE, with GSH catalyzed by GSTπ was identified), and (3) ABL inhibited the nuclear transfer of GSTπ to increase the sensitivity of the nucleus to oxidative stress. These findings suggest that nuclear GSTπ prevents H_2O_2-induced DNA damage by scavenging lipid-peroxide-modified DNA.

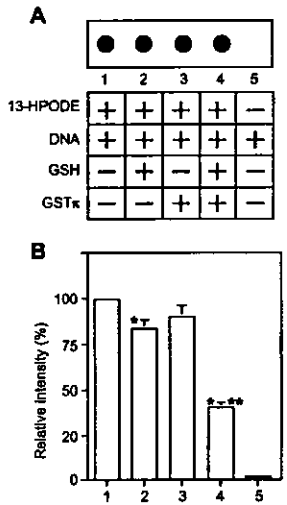

Fig. 7. Effect of GSTπ on the formation of oxo-heptyl-εdG in vitro. (A) 13-HPODE was mixed with $FeCl_2$ and stood for 12 h at 37°C. The solution was incubated with or without GSH and GSTπ in the presence of calf thymus DNA for 1 h at 37°C. DNA extract was spotted on a nitrocellulose membrane and immunologically stained using MAb6A3 as the primary antibody and HRP-conjugated anti-mouse IgG antibody as the secondary antibody. Blots were developed by enhanced chemiluminescence using the ECL kit and the relative immunological activity was analyzed by NIH Image. (B) Relative intensity (%) of the levels of oxo-heptyl-εdG in each lane corresponds to A. Data are the means of three independent analyses. Bars show the SD. $^{*}p < 0.05$ compared with control cells; $^{**}p < 0.05$ compared with H_2O_2-treated cells.

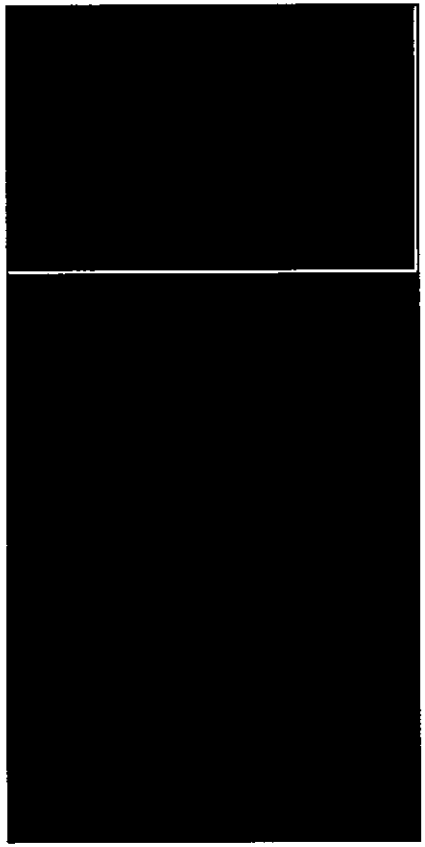

Fig. 8. LC/MS analysis. The chemical structure of the product of the incubation of 13-HPODE and GSH in the presence or absence of GSTπ was characterized by LC/MS. Materials were prepared as described in Fig. 6 legend. (A) 13-HPODE; (B) 13-HPODE with GSH; (C) 13-HPODE with GSH and GSTπ. Arrow indicates 4-ONE-GSH adduct.

Previously, we found that the nuclear GSTπ is an important factor in the acquisition of drug resistance in cancer cells [21,22]. Cancer cells which expressed the nuclear GSTπ in response to anticancer drugs such as DOX and CDDP showed resistance to these drugs, whereas the cells that did not express nuclear GSTπ were more sensitive to the drugs. The conjugation of the drugs with GSH was found in the resistant cells and correlated with decreased drug-induced DNA damage. In the present study, H_2O_2-induced DNA damage was observed when the cells were previously treated with ABL, an inhibitor of the nuclear transfer of GSTπ (Figs. 1–3). Strikingly, HCT8 cells were not sensitive to H_2O_2 (-400 μM). Treatment of the cells with H_2O_2 increased the nuclear transfer of GSTπ in a dose- (data not shown) and time-dependent manner (Fig. 4). The resistance of HCT8 cells to oxidative stress was abolished by pretreatment with ABL. The results strongly suggest an important role for the nuclear GSTπ in the sensitivity of the cells to oxidative stress.

There are many antioxidants in cells. Most of them are localized in the cytoplasm. In addition, each microorgan possesses its own defense system against oxidative stress. A nuclear superoxide dismutase, GPX, and GSTπ have been reported [21,39,40].

Adler et al. [41] reported that GSTp associates with Jun N-terminal kinase (JNK) to regulate its activity in mouse fibroblast NIH3T3 cells. Moreover, Yin et al. [42] demonstrated that GSTp coordinates the activation of extracellular signal-regulated kinases/p38 mitogen-activated protein kinase/inhibitor of κ kinase and suppression of JNK as part of the mechanism underlying its ability to elicit protection against H_2O_2-induced cell death. These findings indicate that GSTp plays an important role in the defense system against oxidative stress through its function as a regulator of stress kinases. It is interesting that GSTp has at least two different functions, to scavenge lipid peroxide and to regulate stress kinases as an antioxidant.

Lipid hydroperoxides are known to be relatively short lived. They are enzymatically and/or nonenzymatically metabolized to stable alcohols in vivo. They also react with metal to form reactive end products

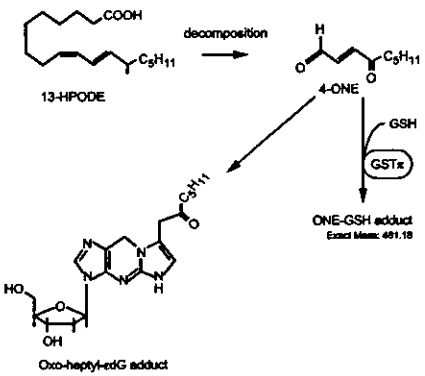

Fig. 9. Schema of the metabolism of 13-HPODE in the nucleus.

such as aldehydes. However, the importance of lipid hydroperoxides to the covalent modifications of biological components has not been thoroughly investigated. oxo-heptyl-ϵdG is formed by the reaction of 13-HPODE with dG [43]. During this reaction, 4-ONE directly mediates the formation of oxo-heptyl-ϵdG [30,43], suggesting that the lipid-hydroperoxide-derived production of 4-ONE contributes to DNA damage. 4-ONE and 4-HNE also form adducts with proteins. These adductions of proteins and DNA are thought to be involved in the pathogenesis of several diseases such as atherosclerosis [44], diabetes mellitus [45], and carcinogenesis [30].

With regard to the reduction of lipid peroxide, reduction of linoleic acid hydroperoxide by GPX was reported [46]. Lipid peroxide once formed is reduced to alcohol by GPX. With regard to the role of GST in the reduction of lipid peroxide, Cao et al. [32] reported that GSH and GST function in protecting against the cytotoxicity of 4-HNE in vascular smooth muscle cells. Depletion of GSH by buthionine sulfoximine and inhibition of GST activity by sufasalazine potentiated the 4-HNE-mediated cytotoxicity. The results suggested that GST functions to form a conjugate of 4-HNE with GSH.

Zimniak et al. [47] reported that mouse GSTA4-4 belongs to the alpha subclass of GST and functions to form a conjugate of 4-HNE with GSH. Additionally, Singhal et al. [48] reported that the human GST corresponding to mouse GSTA4-4 catalyzes the conjugation of 4-HNE with GSH. These reports indicate that GSTA4-4 plays an important role with GSH in the removal of 4-HNE. It is possible that GSTA4-4 functions to form a conjugate of 4-ONE with GSH. On the other hand, the colon cancer cell line employed in the present study possessed mainly GSTπ, which may detoxify 4-HNE and 4-ONE. It has been reported that aldose reductase prevents the formation of 4-HNE [49]. However, there has been no report on the role of GST in the reduction of another lipid peroxidation product, 4-ONE. As shown in Fig. 9, this is the first report to show that GSTπ reduces the formation of DNA adducts with 13-HPODE, characterized as oxo-heptyl-ϵdG. GSTπ catalyzes the conjugation of 4-ONE, a lipid-peroxide-derived product, with GSH, the adduct of which is thought to contribute to age-related diseases or carcinogenesis.

Acknowledgments—We are very grateful to Ms. Junko Takasaki for preparing the manuscript. This work was supported in part by Grants-in-Aid for Scientific Research from the Ministry of Education, Science, Sports, and Culture of Japan.

REFERENCES

[1] Kaneto, H.; Fujii, J.; Suzuki, K.; Kasai, H.; Kawamori, R.; Kamada, T.; Taniguchi, N. DNA cleavage induced by glycation of Cu,Zn-superoxide dismutase. *Biochem. J.* **304**:219–225; 1994.

[2] Nose, K.; Shibanuma, M.; Kikuchi, K.; Kageyama, H.; Sakiyama, T.; Kuroke, T. Transcriptional activation of early-response genes by hydrogen peroxide in a mouse osteoblastic cell line. *Eur. J. Biochem.* **201**:99–106; 1991.

[3] Jakoby, W. B. The glutathione S-transferases: a group of multifunctional detoxification proteins. *Adv. Enzymol. Relat. Areas Mol. Biol.* **46**:383–414; 1978.

[4] Chasseaud, L. F. The role of glutathione and glutathione S-transferases in the metabolism of chemical carcinogens and other electrophilic agents. *Adv. Cancer Res.* **29**:175–274; 1979.

[5] Prohaska, J. R.; Ganther, H. E. Glutathione peroxidase activity of glutathione-S-transferases purified from rat liver. *Biochem. Biophys. Res. Commun.* **76**:437–445; 1977.

[6] Meyer, D. J.; Beale, D.; Tan, K. H.; Coles, B.; Ketterer, B. Glutathione transferases in primary rat hepatomas: the isolation of a form with GSH peroxidase activity. *FEBS Lett.* **184**:139–143; 1985.

[7] Tan, K. H.; Meyer, D. J.; Coles, B.; Ketterer, B. Thymine hydroperoxide, a substrate for rat Se-dependent glutathione peroxidase and glutathione transferase isoenzymes. *FEBS Lett.* **207**:231–233; 1986.

[8] Ujihara, M.; Tsuchida, S.; Satoh, K.; Sato, K.; Urade, Y. Biochemical and immunological demonstration of prostaglandin D_2, E_2, and $F_{2\alpha}$ formation from prostaglandin H2 by various rat glutathione S-transferase isozymes. *Arch. Biochem. Biophys.* **264**:428–437; 1988.

[9] Satoh, K.; Kitahara, A.; Soma, Y.; Inaba, Y.; Hatayama, I.; Sato, K. Purification, induction, and distribution of placental glutathione transferase: a new marker enzyme for preneoplastic cells in the rat chemical hepatocarcinogenesis. *Proc. Natl. Acad. Sci. USA* **82**: 3964–3968; 1985.

[10] Kano, T.; Sakai, M.; Muramatsu, M. Structure and expression of a human class π glutathione S-transferase messenger RNA. *Cancer Res.* **47**:5626–5630; 1987.

[11] Mannervik, B.; Castro, V. M.; Danielson, U. H.; Tahir, M. K.; Hansson, J.; Ringborg, U. Expression of class Π glutathione transferase in human malignant melanoma cells. *Carcinogenesis* **8**:1929–1932; 1987.

[12] Howie, A. F.; Forrester, L. M.; Glancey, M. J.; Schlager, J. J.; Powis, G.; Beckett, G. J.; Hayes, J. D.; Wolf, C. R. Glutathione S-transferase and glutathione peroxidase expression in normal and tumour human tissues. *Carcinogenesis* **11**:451–458; 1990.

[13] Hirata, S.; Odajima, T.; Kohama, G.; Ishigaki, S.; Niitsu, Y. Significance of glutathione S-transferase-π as a tumor marker in patients with oral cancer. *Cancer* **70**:2381–2387; 1992.

[14] Saburi, Y.; Nakagawa, M.; Ono, M.; Sakai, M.; Muramatsu, M.; Kohno, K.; Kuwano, M. Increased expression of glutathione S-transferase gene in cis-diamminedichloroplatinum(II)-resistant variants of a Chinese hamster ovary cell line. *Cancer Res.* **49**: 7020–7025; 1989.

[15] Bai, F.; Nakanishi, Y.; Kawasaki, M.; Takayama, K.; Yatsunami, J.; Pei, X. H.; Tsuruta, N.; Wakamatsu, K.; Hara, N. Immunohistochemical expression of glutathione S-transferase-Π can predict chemotherapy response in patients with nonsmall cell lung carcinoma. *Cancer* **78**:416–421; 1996.

[16] Batist, G.; Tulpule, A.; Sinha, B. K.; Katki, A. G.; Myers, C. E.; Cowan, K. H. Overexpression of a novel anionic glutathione transferase in multidrug-resistant human breast cancer cells. *J. Biol. Chem.* **261**:15544–15549; 1986.

[17] Wang, Y. Y.; Teicher, B. A.; Shea, T. C.; Holden, S. A.; Rosbe, K. W.; al-Achi, A.; Henner, W. D. Cross-resistance and glutathione-S-transferase-π levels among four human melanoma cell lines selected for alkylating agent resistance. *Cancer Res.* **49**:6185–6192; 1989.

[18] Shiratori, Y.; Soma, Y.; Maruyama, H.; Sato, S.; Takano, A.; Sato, K. Immunohistochemical detection of the placental form of glutathione S-transferase in dysplastic and neoplastic human uterine cervix lesions. *Cancer Res.* **47**:6806–6809; 1987.

[19] Ali-Osman, F.; Brunner, J. M.; Kutluk, T. M.; Hess, K. Prognostic significance of glutathione S-transferase π expression and subcellular localization in human gliomas. *Clin. Cancer Res.* **3**:2253–2261; 1997.

[20] Yu, L. G.; Fernig, D. G.; White, M. R. H.; Spiller, D. G.; Appleton, P.; Evans, R. C.; Grierson, I.; Smith, J. A.; Davies, H.; Gerasimenko, O. V.; Petersen, O. H.; Milton, J. D.; Rhodes, J. M. Edible mushroom (*Agaricus bisporus*) lectin, which reversibly inhibits epithelial cell proliferation, blocks nuclear localization sequence-dependent nuclear protein import. *J. Biol. Chem.* **274**:4890–4899; 1999.

[21] Goto, S.; Ihara, Y.; Urata, Y.; Izumi, S.; Abe, K.; Koji, T.; Kondo, T. Doxorubicin-induced DNA intercalation and scavenging by nuclear glutathione S-transferase pi. *FASEB J.* **14**:2702–2714; 2001.

[22] Goto, S.; Kamada, K.; Soh, Y.; Ihara, Y.; Kondo, T. Significance of nuclear glutathione S-transferase pi in resistance to anti-cancer drugs. *Jpn. J. Cancer Res.* **9**:1047–1056; 2002.

[23] Burcham, P. C. Genotoxic lipid peroxidation products: their DNA damaging properties and role in formation of endogenous DNA adducts. *Mutagenesis* **13**:287–305; 1998.

[24] Marnett, L. J. Lipid peroxidation-DNA damage by malondialdehyde. *Mutat. Res.* **424**:83–95; 1999.

[25] Seto, H.; Okuda, T.; Takesue, T.; Ikemura, T. Reaction of malondialdehyde with nucleic acid. I. Formation of fluorescent pyrimido[1,2-a]purin-10 (3*H*)-one nucleosides. *Bull. Chem. Soc. Jpn.* **56**:1799–1802; 1983.

[26] Winter, C. K.; Segall, H. J.; Haddon, W. F. Formation of cyclic adducts of deoxyguanosine with the aldehydes *trans*-4-hyroxy-2-hexenal and trans-4-hydroxy-2-nonenal in vitro. *Cancer Res.* **46**: 5682–5686; 1986.

[27] Chung, F.-L.; Young, R.; Hecht, S. S. Formation of cyclic 1, N^2-propanodeoxyguanosine adducts in DNA upon reaction with acrolein or crotonaldehyde. *Cancer Res.* **44**:990–995; 1984.

[28] Wang, M.-Y.; Liehr, J. G. Lipid hydroperoxide-induced endogenous DNA adducts in hamsters: possible mechanism of lipid hydroperoxide-mediated carcinogenesis. *Arch. Biochem. Biophys.* **316**:38–46; 1995.

[29] Inouye, S. Site-specific cleavage of double-strand DNA by hydroperoxide of linoleic acid. *FEBS Lett.* **172**:231–234; 1984.

[30] Kawai, Y.; Kato, Y.; Nakae, D.; Kusuoka, O.; Konishi, Y.; Uchida, K.; Osawa, T. Immunohistochemical detection of a substituted 1,N^2-ethenodeoxyguanosine adduct by ω-6 polyunsaturated fatty acid hydroperoxides in the liver of rats fed a choline-deficient, L-amino acid-defined diet. *Carcinogenesis* **3**:485–489; 2002.

[31] Doorn J. A.; Petersen, D. R. Covalent adduction of nucleophilic amino acids by 4-hydroxynonenal and 4-oxononenal. *Chem. Biol. Interact.* **1**:143–144: 93–100; 2003.

[32] Cao, Z.; Hardej, D.; Trombetta, L. D.; Li, Y. The role of chemically induced glutathione and glutathione S-transferase in protecting against 4-hydroxy-2-nonenal-mediated cytotoxicity in vascular smooth muscle cells. *Cardiovasc. Toxicol.* **3**:165–177; 2003.

[33] Gong, J.; Traganos, F.; Darzynkiewicz, Z. A. Selective procedure for DNA extraction from apoptotic cells applicable for gel electrophoresis and flow cytometry. *Anal. Biochem.* **218**:314–319; 1994.

[34] Dignam, J. D.; Lebovitz, R. M.; Roeder, R. G. Accurate transcription initiation by RNA polymerase II in a soluble extract from isolated mammalian nuclei. *Nucleic Acids Res.* **11**:1475–1489; 1983.

[35] Goto, S.; Iida, T.; Cho, S.; Oka, M.; Kohno, S.; Kondo, T. Overexpression of glutathione S-transferase π enhances the adduct formation of cisplatin with glutathione in human cancer cells. *Free Radic. Res.* **31**:549–558; 1999.

[36] Redinbaugh, M. G.; Turley, R. B. Adaptation of the bicinchoninic acid protein assay for use with microtiter plates and sucrose gradient fractions. *Anal. Biochem.* **153**:267–271; 1986.

[37] Abmayr, S. M.; Workman, J. L. *DNA-protein interactions*. In: Ausubel, F. M.; Brent, R.; Kingston, R. E.; Moore, D. D.; Seidman, J. G.; Smith, J. A.; Struhl, K., eds. Current protocols in molecular biology. Vol. 11. New York: Greene Publishing Asociates and Willey-Interscience. 1203–1219; 1987

[38] Ohkawa, H.; Ohishi, N.; Yagi, K. Assay for lipid peroxides in animal tissues by thiobarbituric acid reaction. *Anal. Biochem.* **95**:351–358; 1979.

[39] Ookawara, T.; Kizaki, T.; Takayama, E.; Imazeki, N.; Matsubara, O.; Ikeda, Y.; Suzuki, K.; Li Ji, L.; Tadakuma, T.; Taniguchi, N.; Ohno, H. Nuclear translocation of extracellular superoxide dismutase. *Biochem. Biophys. Res. Commun.* **296**:54–61; 2002.

[40] Nakamura, T.; Imai, H.; Tsunashima, N.; Nakagawa, Y. Molecular cloning and functional expression of nucleolar phospholipid hydroperoxide glutathione peroxidase in mammalian cells. *Biochem. Biophys. Res. Commun.* **311**:139–148; 2003.

[41] Adler, V.; Yin, Z.; Fuchs, S. Y.; Benezra, M.; Rosario, L.; Tew, K. D.; Pincus, M. R.; Sardana, M.; Henderson, C. J.; Wolf, C. R.; Davis, R. J.; Ronai, Z. Regulation of JNK signaling by GSTp. *EMBO J.* **18**:1321–1334; 1999.

[42] Yin, Z.; Vladimir, N. I.; Hasem, H.; Kenneth, T.; Ronai, Z. Glutathione S-transferase p elicits protection against H_2O_2-induced cell death via coordinated regulation of stress kinases. *Cancer Res.* **60**:4054–4057; 2000.

[43] Rindgen, D.; Nakajima, M.; Wehrli, S.; Xu, K.; Blair, I. A. Covalent modifications to 2′-deoxyguanosine by 4-oxo-2-nonenal, anovel product of lipid peroxidation. *Chem. Res. Toxicol.* **12**:1195–1204; 1999.

[44] Rosenfeld, M. E.; Palinski, W.; Yla-Herttuala, S.; Butler, S.; Witztum, J. L. Distribution of oxidation specific lipid-protein adducts and apolipoprotein B in atherosclerotic lesions of varying severity from WHHL rabbits. *Arteriosclerosis* **10**:336–349; 1990.

[45] Yamanouchi, J.; Takatori, A.; Itagaki, S.; Kawamura, S.; Yoshikawa, Y. APA hamster model for diabetic atherosclerosis. 2. Analysis of lipids and lipoproteins. *Exp. Anim.* **49**:267–274; 2000.

[46] Little, C.; O'Brien, P. J. An intracellular GSH-peroxidase with a lipid peroxide substrate. *Biochem. Biophys. Res. Commun.* **31**: 145–150; 1968.

[47] Zimniak, P.; Singhal, S. S.; Srivastava, S. K.; Awasthi, S.; Sharma, R.; Hyden, J. B.; Awasthi, Y. C. Estimation of genomic complexity, heterologous expression, and enzymatic characterization of mouse glutathione S-transferase mGSTA4-4 (GST5.7). *J. Biol. Chem.* **269**:992–1000; 1994.

[48] Singhal, S. S.; Zimniak, P.; Awasthi, S.; Piper, J. T.; He, N. G.; Teng, J. I.; Petersen, D. R.; Awasthi, Y. C. Several closely related glutathione S-transferase isozymes catalyzing conjugation of 4-hydroxynonenal are differentially expressed in human tissues. *Arch. Biochem. Biophys.* **311**:242–250; 1994.

[49] Vander Jagt, D. L.; Kolb, N. S.; Vander Jagt, T. J.; Chino, J.; Martinez, F. J.; Hunsaker, L. A.; Royer, R. E. Substrate specificity of human aldose reductase: identification of 4-hydroxynonenal as an endogenous substrate. *Biochim. Biophys. Acta* **1249**:117–126; 1995.

ABBREVIATIONS

ABL—edible mushroom (*Agaricus bispourus*) lectin
GPX—glutathione peroxidase
GSH—reduced form of glutathione
GST—glutathione *S*-transferase
LC/MS—liquid chromatography/mass spectrometry
Oxo-heptyl-ϵdG—7-(2 oxo-hepyl)-substituted 1,N^2-etheno-2′-deoxyguanosine adduct
TBARS—thiobarbituric acid reactive substance
TUNEL—terminal deoxynucleotidyl transferase-mediated dUTP nick end labeling
4-HNE—4-hydroxy-2-nonenal
4-ONE—4-oxo-2-nonenal
13-HPODE—13-hydroperoxyoctadecadienoic acid

Free Radical Biology & Medicine, Vol. 32, No. 8, pp. 688–701, 2002

0891-5849/02/$–see front matter

ELSEVIER

PII S0891-5849(01)00823-1

Original Contribution

REACTIVE OXYGEN SPECIES ACCELERATE PRODUCTION OF VASCULAR ENDOTHELIAL GROWTH FACTOR BY ADVANCED GLYCATION END PRODUCTS IN RAW264.7 MOUSE MACROPHAGES

YOSHISHIGE URATA,* MICHIKO YAMAGUCHI,† YASUHITO HIGASHIYAMA,* YOSHITO IHARA,* SHINJI GOTO,* MICHIHIKO KUWANO,‡ SEIKOH HORIUCHI,§ KOJI SUMIKAWA,† and TAKAHITO KONDO*

*Department of Biochemistry and Molecular Biology in Disease, Atomic Bomb Disease Institute and †Department of Anesthesiology, Nagasaki University School of Medicine, Nagasaki, Japan; ‡Department of Biochemistry, Kyushu University School of Medicine, Maidashi, Fukuoka, Japan; and §Department of Biochemistry, Kumamoto University School of Medicine, Kumamoto, Japan

(*Received* 10 *October* 2001; *Accepted* 13 *December* 2001)

Abstract—Advanced glycation end products (AGEs) are believed to play an important role in the development of angiopathy in diabetes mellitus. Previous reports suggested a correlation between accumulation of AGEs and production of vascular endothelial growth factor (VEGF) in human diabetic retina. However, the mechanisms involved were not revealed. In this study, we investigated the transcriptional regulation of the expression of vascular endothelial growth factor (VEGF) by AGEs, and possible involvement of reactive oxygen species (ROS) in the induction. We employed an AGE of bovine serum albumin (BSA) prepared by an incubation of BSA with D-glucose for 40 weeks and N(epsilon)-(carboxymethyl)lysine (CML), a major AGE. The expression of VEGF was induced by CML-BSA in RAW264.7 mouse macrophage-like cells. CML-BSA stimulated the DNA-binding activity of activator protein-1 (AP-1). Promoter assay showed that the induction of VEGF was dependent on AP-1. The activity of Ras/Raf-1/MEK/ERK1/2 was involved in the CML-BSA-stimulated signaling pathways to activate the AP-1 transcription with a peak at 1 h. AGE-BSA also induced VEGF mediated by AP-1, however, there was a difference of effect between AGE-BSA and CML-BSA in the activation of AP-1. AGE-BSA-stimulated AP-1 activity showed a peak at 5 h, which paralleled the formation of ROS. Reduction of AGE-BSA with $NaBH_4$ or addition of vitamin E attenuated the AGE-BSA-stimulated signaling pathways leading to the same pattern as for CML-BSA-stimulated signals. These results suggest an important role for AGEs in stimulation of the development of angiogenesis observed in diabetic complications, and that ROS accelerates the AGE-stimulated VEGF expression.

Keywords—ROS, AGE, CML, VEGF, ANG, ERK1/2, AP-1, RAW264.7 cells, Free radicals

INTRODUCTION

Advanced glycation end products (AGEs) are applied to a broad range of advanced products of the Mailard reaction, such as N-(carboxymethyl) hydroxylysine, pyraline, pentosidine, and crosslines. Glucose binds to proteins and forms early glycation products such as Schiff base and Amadori products, and later AGEs in the Maillard reaction. AGEs are nonenzymatically glycated and autooxidized proteins [1]. Reactive oxygen species (ROS) are produced in the Maillard reaction [2] and help to form AGEs [3]. On incubation of glucose with proteins, a reactive intermediate such as glycoaldehyde, glyoxal, or methylglyoxal diimine forms, and is converted to a N(epsilon)-(carboxymethyl)lysine (CML)-modified protein. CML-adducts are the predominant AGE in vivo, especially in vascular tissue, atherosclerotic lesions, and glomerular tissue retrieved from diabetic rodents and human subjects [4–9].

Vascular macrophages play a role in the progression of the vascular injury [10], which develops during the progression of diabetes mellitus (DM). These cells uptake AGEs through receptors, such as AGE-specific cell surface receptors (RAGEs) [4,10], macrophage scavenger receptor-A, or galectin-3 [11]. The uptake of CML adducts by macrophages also occurs through these RAGEs [4,10,12].

Neovascularization is induced by potent angiogenic factors such as Vascular Endothelial Growth Factor (VEGF)/Vascular Permeability Factor, angiogenin (ANG), and basic fibroblast growth factor (bFGF). VEGF plays a key role in angiogenesis and vascular permeability. VEGF was purified from bovine pituitary folliculostellate cells [13,14]. The human gene for VEGF and its promoter region was cloned and characterized by Tischer et al. [15]. VEGF mRNA is highly expressed and produced in various tissue cells such as vascular endothelial cells, vascular smooth muscle cells, macrophages, and some tumor cells [16]. VEGF mRNA levels are thought to be closely related to neovascularization and the progression of angiopathies [17]. Tsuchida et al. reported the effect of an AGE inhibitor on the expression of VEGF and transforming growth factor-β in diabetic nephropathy in rats [18]. Analysis of the VEGF promoter region reveals several potential binding sites for oxidative stress-responsive transcription factors such as activator protein (AP)-1, AP-2, specificity protein-1 (Sp1), and nuclear factor-κB (NF-κB) [15,19].

CML adducts bound to RAGEs activate NF-κB to modulate gene expression [4]. Mitogen-activated protein kinases (MAPKs) are involved in the RAGE-mediated signal pathways leading to stimulation of the NF-κB transcriptional activity [20]. Our group previously reported a relation between accumulation of CML adducts and VEGF expression in diabetic retina [21]. The data suggests that VEGF is induced by CML adducts, however, the signal pathways by which VEGF mRNA is induced by CML adducts have not been clarified.

ANG derived from a tumor-derived potent angiogenic factor [22] has 35% sequence identity with human pancreatic ribonuclease and is a polypeptide with a molecule size of 14 kD. The action of ANG is thought to be mediated through a specific cell surface receptor on endothelial cells [23], even though the exact mechanism for the induction of neovascularization by ANG is still not known. An increase in the level of ANG has been reported in serum from diabetic patients [24], and vitreous from patients with proliferative diabetic nephropathy [25].

In addition to our previous report on the accumulation of CML in human diabetic retina [21], Hammes et al. reported that intracellular accumulation of CML in long-lived T-lymphocytes is a marker of microvascular complication of DM [26]. These reports suggest that VEGF and/or ANG, potent angiogenic factors possibly induced by CML adducts, contribute to the development of diabetic complications.

The interaction of AGEs with RAGEs leads to oxidative stress at the cell surface and the formation of ROS [27]. Furthermore, stimulation of Ras leads to activation of Raf-1 kinase and MAPKs, and production of ROS [28]. Activation of NADPH oxidase leading to production of ROS is also observed in response to growth factors such as transforming growth factor (TGF-α) [29] and angiotensin-II [30], while TGF-β does not produce ROS [29]. It is well known that the transcriptional activities of AP-1, NF-κB, STAT1, and Elk1 are stimulated by MAPKs and these activities are responsive to oxidative stress. However, the importance of ROS in the intracellular signal pathways mediated by AGEs is not fully understood. In the present study, we studied the transcriptional regulation of VEGF expression induced by AGE adducts and found evidence that the adducts stimulate the DNA-binding activity of AP-1 leading to induction of VEGF mRNA. We found that ROS produced by glucose-derived AGEs stimulates the activity of Ras/Raf/MEK/ERK1/2, however, ROS is involved in CML-bovine serum albumin (BSA)-mediated signals to a lesser degree. These results suggested an important role for AGEs in stimulation of the development of angiogenesis observed in diabetic complications, and formation of ROS by AGEs accelerates the AGE-stimulated VEGF expression.

MATERIALS AND METHODS

Materials

RAW264.7 mouse macrophage cells were purchased from the Health Sciences Research Resources Bank (Tokyo, Japan). The cells were maintained in Dulbecco's Modified Eagle's Medium (DMEM) supplemented with 10% fetal calf serum at 37°C in 5% CO_2 and 100% humidity. Human VEGF121 cDNA [31] was kindly donated by H. A. Weich (Department of Gene Regulation and Differentiation, National Center for Biotechnology, Braunschweig, Germany). Trolox was purchased from the OXIS international, Inc. (Portland, OR, USA).

AGEs were prepared under sterilized condition. CML-BSA was prepared as described previously [32]. Briefly, 2 mg/ml of BSA was incubated at 37°C for 24 h with 0.75 mol/l glyoxylic acid and 0.3 mol/l $NaCNBH_3$ in 0.5 mol/l sodium phosphate buffer, pH 7.4. This was followed by dialysis against phosphate-buffered saline (PBS). In this CML-BSA preparation, the extent of modification was 34.5 mol of CML/mol of BSA. AGE-BSA was prepared as described previously [32]. Briefly, BSA (1.6 g) was incubated with D-glucose (3.0 g) in 10 ml of 0.5 mol/l sodium phosphate buffer, pH 7.4, at 37°C for 40 weeks, and then dialyzed against phosphate-buffered saline. As a control, BSA was in parallel incubated without D-glucose for 40 weeks. In this AGE-BSA preparation, 40 out of 59 lysine residues were modified, of

Address correspondence to: Takahito Kondo, M.D., Ph.D., Professor and Chairman, Department of Biochemistry and Molecular Biology in Disease, Atomic Bomb Disease Institute, Nagasaki University School of Medicine, Nagasaki 852-8523, Japan; Tel: +81 (95) 849-7099; Fax: +81 (95) 849-7100; E-Mail: kondo@net.nagasaki-u.ac.jp.

which 9 mol were CML adducts. Namely, the extent of CML modification of AGE-BSA preparation was 9 mol/mol of BSA. Reactive glycation intermediates were reduced by treating with 50 mM sodium borohydride ($NaBH_4$) for 1 h [33]. Possible contamination of bacterias was not observed microscopically in the incubation medium for RAW264.7 cells with AGEs for 3 d.

Northern blots

The cloned cDNA was isolated as described by Godwin et al. [34]. A VEGF probe (721 bp corresponding to nucleotides 141–861 of human VEGF homologous to mouse VEGF) was generated from human umbilical vein endothelial cells. Isolation of cytoplasmic RNA and Northern blotting were essentially performed as described by Sambrook et al. [35]. Cytoplasmic RNAs isolated from RAW264.7 cells were subjected to electrophoresis in 1% agarose gels containing 0.6 M formaldehyde, subsequently transferred to nylon membranes, and then hybridized with ^{32}P-labeled probes. Autoradiographed membranes were analyzed using a Fujix Bio-Analyzer BAS-5000 (Fuji Photo Film, Tokyo, Japan). After being stripped, the membranes were rehybridized with ^{32}P-labeled glyceraldehyde-3-phosphate dehydrogenase (GAPDH) probe. The relative radioactivity was expressed as a ratio of photostimulated luminescence (PSL) corrected by the intensity of GAPDH.

Preparation of cDNA

Cloning of mouse ANG and mouse bFGF was performed using an RNA PCR kit (TAKARA SHUZO CO Ltd., Tokyo, Japan) according to a commercial protocol. Template RNA was prepared using RNeasy mini kits (Qiagen Co. Ltd., Hilden, Germany) from RAW264.7 cells. The authentic sense primer for ANG was 5′-ATGGCGATAAGCCCAGGCCCG-3′ and the antisense primer was 5′-CTATAGACTGAAAAATGACTCATCGAAGTG-3′. The authentic sense primer for bFGF was 5′-TTGGCTGCCAGCGGAATCACC-3′ and the antisense primer was 5′-TCAGCTCTTAGCAGACATTGG-3′. The cDNAs obtained were of 438 base pairs (bp) corresponding to bp 1–438 of mouse ANG and 465 bp corresponding to bp 1–465 of mouse bFGF.

Semiquantitative RT-PCR

Semiquantitative RT-PCR for the estimation of the levels of ANG and bFGF mRNAs was performed using an RNA PCR kit with 25 cycles for ANG and 35 cycles for bFGF. Levels of β-actin was used as an internal standard. The products of RT-PCR were subjected to electrophoresis in 1% agarose gels, subsequently transferred to nylon-membrane filters, and later hybridized with ^{32}P-labeled probes for these genes. Autoradiographed filters were analyzed using a Fujix Bio-Analyzer BAS-5000 (Fuji Photo Film).

Preparation of nuclear extract

Nuclear extracts were prepared as described by Abmayr and Workman [36]. Briefly, the cells were suspended in hypotonic buffer, 10 mM HEPES, pH 7.9, containing 1.5 mM $MgCl_2$, 10 mM KCl, 0.2 mM phenylmethylsulfonyl fluoride (PMSF), and 0.5 mM dithiothreitol (DTT). The swollen cells were homogenized and the nuclei pelleted. The soluble nuclear proteins were prepared by adding a high-salt buffer, 20 mM HEPES, pH 7.9, containing 25% glycerol, 1.5 mM $MgCl_2$, 1.2 M KCl, 0.2 mM EDTA, 0.2 mM PMSF, and 0.5 mM DTT followed by centrifugation.

Electrophoretic mobility shift assay

The electrophoretic mobility shift assay for AP-1 was performed as described by Sen and Baltimore [37] with a slight modification. Briefly, nuclear extracts were incubated with ^{32}P-oligonucleotide specific for AP-1. The binding reaction proceeded in a 20-μl reaction mixture containing 10 μg of extract, 4 μl of a binding buffer (10 mM Tris, pH 7.5, 40 mM NaCl, 1 mM EDTA, 1 mM 2-mercaptoethanol, 4% glycerol), 2 μg of poly (dI-dC) as a nonspecific competitor DNA, 2 μg of BSA and labeled oligonucleotide (3000–6000 cpm). After a 30 min binding reaction at room temperature, samples were loaded on a 6% nondenaturing polyacrylamide gel and subjected to electrophoresis in 50 mM Tris, 45 mM borate, and 0.5 mM EDTA, pH 8.0. As a specificity control, a 100-fold excess of unlabeled probe was applied. The sequence for the binding was prepared according to the nucleotide sequence of the mouse VEGF promoter region containing 5′—TGAGTGA—3′ for the AP-1 probe.

Decoy approach

The decoy approach was used as described by von Knethen et al. [38]. Briefly, as an AP-1 decoy, a *cis*-element double-stranded oligodeoxynucleotide was synthesized with 5′-CCGCCACTGACTAACTCCAG-3′ and 3′-GGCGGTGACTGATTGAGGTC-5′. RAW264.7 cells were exposed to the AP-1 decoy or vehicle (control). One day before transfection, cells were seeded at a density of 1×10^6/well in to six-well plates. Three micromolar decoy oligonucleotides were added 24 h before the treatment with AGE. After changing the medium, CML-BSA was added for 1 h for the electrophoretic mobility shift assay of AP-1, and 6 h for Northern blotting of VEGF mRNA.

CAT assay of VEGF promoter

The human VEGF promoter and 5′-deletion constructs were used for the transfection of RAW264.7 cells. Synthetic oligonucleotides (20-mer) were prepared on the basis of the published DNA sequence of the VEGF promoter region as described [19]. The reporter plasmids for expression in RAW264.7 cells were obtained as follows. The *Nde* I-*Bam* HI VEGF promoter fragment was cloned into the *Hind* III linkers and designated V1. VEGF promoter deletions from −624 to +430 were constructed [19]. The promoter fragment was obtained from a subclone, and fragments from −268, −129, −94, or −49 to +430 were isolated and designated V2-5, respectively. Site-directed mutagenesis of AP-1 was performed using a LAPCR in vitro Mutagenesis Kit (TAKARA SHUZO Ltd.). The sequence of the AP-1 binding site from −490 bp to −484 bp was changed from 5′-TGAGTGA-3′ to TGAGTTG-3′ and designated V6. RAW264.7 cells were transfected with a mixture of VEGF-CAT construct (10 μg) and β-galactosidase construct (0.5 μg) by a calcium co-precipitation method [19]. Each CAT assay was performed using identical amounts of protein as described previously [39]. The CAT activities of the transient transfection assay were normalized to β-galactosidase activity. The activity of β-galactosidase was estimated according to the method described by Rosenthal [40].

Immune complex kinase assay

The phosphorylation of a mitogen-activated protein kinase (MAPK), such as the extracellular signal-regulated kinases 1 and 2 (ERK1/2, p44/p42), c-Jun N-terminal kinase (JNK, p54/p46), and p38^{MAPK}, was measured as described in the protocol supplied by New England BioLabs (Beverly, MA, USA), using phospho-specific antibodies against phosphorylated sites of ERK1/2, JNK, and p38^{MAPK}. Non-phospho-specific antibodies against ERK1/2, JNK, and p38^{MAPK} proteins provided in each assay kit were used to normalize the phosphorylation assay by using the same transferred membrane blot. The phosphorylated forms of proteins were detected by ECL chemiluminescence. Raf-1 kinase activity was measured using [γ-^{32}P]ATP (3000 Ci/mmol, Amersham Pharmacia Biotech, Buckinghamshire, UK) and Purified MEK-1 protein (Santa Cruz Biotechnology, Inc., Santa Cruz, CA, USA) according to the method described by Egea et al. [41]. Briefly, cells were washed twice with ice-cold PBS and lysed in Triton lysis buffer (25 mM Tris, pH 8.0, 137 mM NaCl, 1% Triton X-100, 10% glycerol) containing protease and phosphatase inhibitors (PMSF/aprotinin/pepstatin and sodium orthovanadate/sodium fluoride). For kinase assay, cell extracts (50 μg) were incubated with 0.5 μg of antibody against Raf-1 (Santa Cruz Biotechnology). After incubation for 2 h at 4°C, 30 μl of protein A-agarose was added and incubated for an additional 30 min. Raf immunocomplexes were washed three times with Triton lysis buffer and twice with MEK buffer (25 mM HEPES, pH 7.4, 10 mM $MgCl_2$, 100 mM NaCl, 1 mM dithiothreitol, 5 μM ATP). Immune complexes were then incubated in 40 μl of kinase buffer containing 20 μCi [γ-^{32}P]ATP and 0.5 μg of MEK-1 for 30 min at room temperature. Reactions were terminated by the addition of 40 μl of 2× Laemmli sample buffer and boiling for 5 min. Reaction products were separated by SDS-PAGE (10% gel). After drying the gel, the phosphorylation signal was analyzed using BAS5000 (Fuji Photo Film).

Estimation of ROS

The production of ROS after the cells had been incubated with CML-BSA was estimated fluorometrically using 2′,7′-dichlorofluorescein diacetate (DCFH-DA) as the substrate according to the method of Bass et al. [42] in a FACScan flow cytometer (Becton-Dickinson, San Jose, CA, USA). Unless otherwise indicated, cells (2×10^6) previously incubated with AGEs were treated with 5 μM DCFH-DA for 30 min at 37°C. The formation of 2′,7′-dichlorofluorescein was determined by flow cytometry. An argon-ion laser was used at an excitation wavelength of 488 nm, and green fluorescence collected through a 530 nm band-pass filter was measured on a logarithmic scale. The formation of ROS is expressed as relative fluorescence intensity (%).

Statistical analysis

The data are given as the mean ± SD. Differences were calculated with Student's two-tailed *t*-test, otherwise with one-way Fractional ANOVA test. Significance was taken as $p < .05$ for Student's *t*-test and $p < .0001$ for Fractional ANOVA test, respectively.

RESULTS

Expression of VEGF mRNA

The effect of AGEs on the expression of VEGF was determined using RAW264.7 mouse macrophages. Figure 1 shows the results of Northern blot analysis for

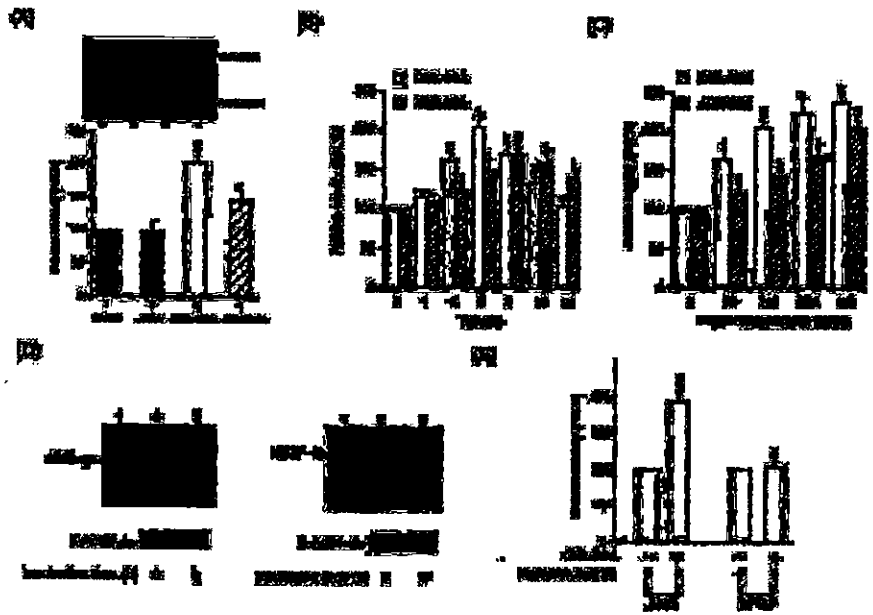

Fig. 1. Induction of VEGF mRNA by AGEs. The effect of CML-BSA on the expression of VEGF mRNA was examined. The expression of VEGF mRNA was estimated from Northern blots. RAW264.7 cells were treated with AGEs and RNAs were prepared after 6 h (A). Control (lane 1), 100 μg/ml of nontreated BSA (lane 2), 100 μg/ml of CML-BSA (lane 3), and 200 μg/ml of AGE-BSA (lane 4). The effect of incubation time (B) and dose-dependent effect of AGEs for 6 h (C) were estimated in RAW264.7 cells. Values were normalized to the GAPDH mRNA level and were expressed as relative intensity (PSL%), taking the level of VEGF in normal RAW264.7 cells as 100%. Open bar, CML-BSA; dashed bar, AGE-BSA. (D) Effect of CML-BSA on the expression of ANG and bFGF was analyzed by semiquantitative RT-PCR. RAW264.7 cells were treated with CML-BSA and RNAs were prepared after 6 h (D), Standard (lane 1), 100 μg/ml of CML-BSA at 0 h (lane 2) and at 6 h (lane 3). (E) The data were obtained as relative intensity (PSL%). The expression of ANG and bFGF was corrected with that of β-actin taking the level of ANG and bFGF at 0 h as 100%. Data are the mean ± SD (%) of three independent analyses. $^{*}p < .01$ vs. each control.

VEGF mRNA. Taking the relative intensity of VEGF mRNA in the cells before the treatment as 100%, that in the cells treated with 100 μg/ml of CML-BSA for 6 h was 205 ± 2.5%, and with 200 μg/ml of AGE-BSA was 150 ± 1.8% (mean of three independent analyses). Non-modified BSA did not induce the expression of VEGF mRNA (Fig. 1A).

Next, the effect of incubation time and dose of AGEs on the levels of VEGF mRNA were estimated. The time course study (Fig. 1B) showed that the expression of VEGF mRNA increased of the treatment with 100 μg/ml of CML-BSA, showed a peak in the 6th hour, and was reduced in the 9th hour. Treatment of the cells with 200 μg/ml of AGE-BSA increased the expression of VEGF mRNA, with a peak in the 9th hour, and the increase continued for 24 h. The induction of VEGF by these AGEs was dose-dependent (Fig. 1C). Approximately 4-fold the concentration of AGE-BSA was required for the expression of VEGF mRNA induced by CML-BSA. Figure 1D shows the results of semiquantitative RT-PCR for ANG and bFGF. CML-BSA produced ANG mRNA (200 ± 15%) but not bFGF mRNA.

An electrophoretic mobility shift assay

Figure 2 shows the results of an electrophoretic mobility shift assay for AP-1 of the VEGF promoter. Treatment of the cells with 100 μg/ml of CML- BSA stimulated the AP-1-DNA binding activity within 1 h and the stimulatory effect declined in 3 h (lanes 5 and 6). Treatment of the cells with 200 μg/ml of AGE- BSA stimulated the AP-1-DNA binding activity within 1 h and the

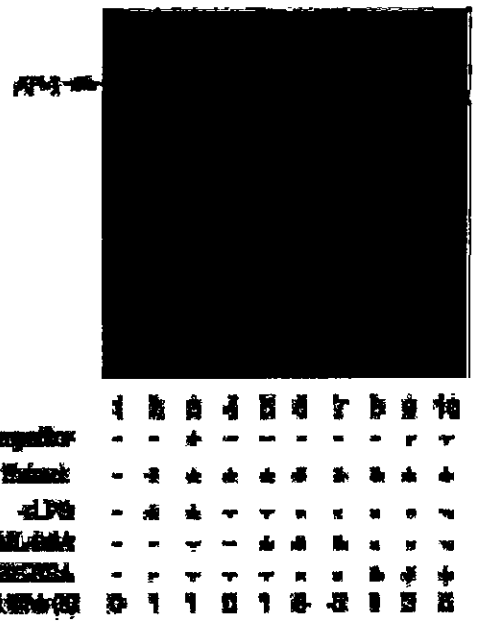

Fig. 2. Electrophoretic mobility shift assay of AP-1. The effect of AGEs on the activity was studied. RAW264.7 cells were treated with 100 μg/ml of CML-BSA or 200 μg/ml of AGE-BSA and nuclear extracts at the times indicated were incubated with an AP-1-specific ^{32}P-oligonucleotide for 30 min and then loaded on a 6% nondenaturing polyacrylamide gel. The DNA binding activities of the extracts were estimated by electrophoretic mobility shift assay. AP-1 activity; lane 1, free probe; lanes 2–10, cell-nuclear extracts from RAW264.7 cells; lanes 2 and 3, + 100 ng/ml of LPS as a positive control; lane 3, + competitor for AP-1; lanes 4–7, + 100 μg/ml of CML-BSA for 0 h (lane 4), 1 h (lane 5), 3 h (lane 6), and 5 h (lane 7); lanes 8–10, + 200 μg/ml of AGE-BSA for 1 h (lane 8), 3 h (lane 9), and 5 h (lane 10).

stimulatory effect continued and showed a peak of activity at 5 h (lanes 8–10).

The CAT activity of the VEGF promoter

We constructed chimeric genes containing various regions of the VEGF gene promoter. RAW264.7 cells were transiently transfected with pSV00CAT containing the VEGF promoter construct. CAT activity stimulated by 100 μg/ml of CML- BSA was found in the VEGF promoter containing the AP-1 binding site (Fig. 3, lane V1). Deletion (lane V2) and mutagenesis of the AP-1 site (lane V6) abolished the CAT activity stimulated by CML-BSA. This strongly suggests that CML-BSA stimulates the transcription of the VEGF gene mediated by AP-1. The effect of AGE-BSA on the CAT activity was the same as that of CML-BSA (data not shown).

MAPK activity

MAPKs are known to be involved in the activation of AP-1. Next, we confirmed whether the MAPK signal pathway is involved in the induction of VEGF mediated by AP-1. Figure 4A shows the effect of AGEs on the activity of ERK1/2. The level of phosphorylated ERK1/2 was elevated 30 min after the treatment with 100 μg/ml of CML- BSA, and showed a peak at 60 min. The AGE-BSA-mediated stimulation of ERK1/2 showed a peak at 60–90 min and continued for over 120 min. Figure 4B shows that other MAPKs such as JNK (p54/p46) and $p38^{MAPK}$ were not stimulated by CML-BSA,

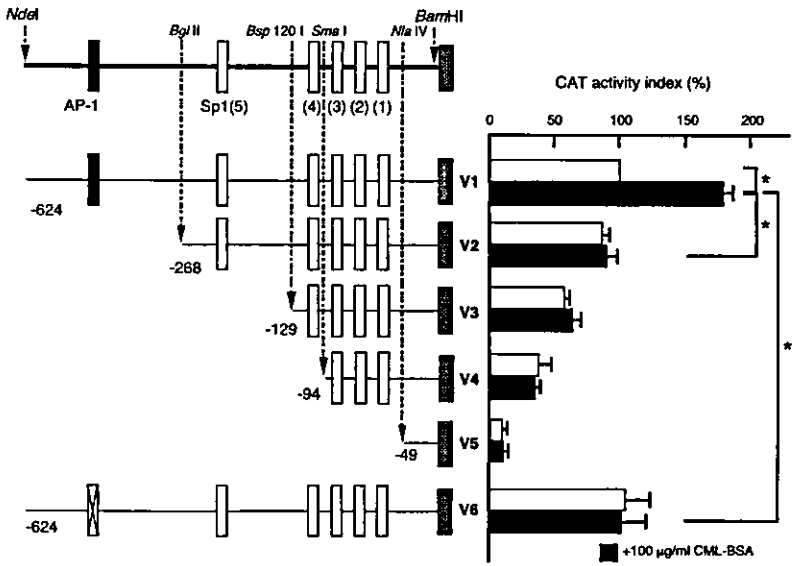

Fig. 3. CAT activity of VEGF promoter. RAW264.7 cells were transiently transfected with a VEGF promoter-CAT gene fusion plasmid. The cells were treated with 100 μg/ml of CML-BSA and incubated for 6 h. Putative sequences in the 5′-upstream region of the human VEGF gene and restriction enzymes used are illustrated (upper left). Numbers indicate the distance in base pairs from the start of transcription. V1, a *Nde* I-*Bam* HI fragment of VEGF promoter; V2, V1 lacking AP-1; V3, V1 lacking AP-1 and Sp1 (5); V4, V1 lacking AP-1, Sp1 (5) and Sp1 (4); V5, V1 lacking AP-1 and Sp1 (1-5); V6, V1 with a mutation at the AP-1 site. The CAT activity was corrected for differences in transfection efficiency among the cells as estimated from β-galactosidase activity and then normalized to the corrected activity of cells transiently transfected with VEGF-CAT. The relative fold-increase was determined from values normalized to the endogenous CAT activity of the transfected cells in the absence of CML-BSA. Data are the mean ± SD (%) of three independent analyses. $^{*}p < .01$.

and AGE-BSA stimulated the activity of ERK1/2 and JNK, but not that of $p38^{MAPK}$.

AP-1 decoy approach

To further affirm the role of AP-1 activity in the induction of VEGF by AGEs, an AP-1 decoy approach was used. Figure 5 shows the effect of the AP-1 decoy on the VEGF mRNA expression induced by AGEs. Pretreatment of RAW264.7 cells with 3 μM AP-1 decoy completely abolished the CML-BSA-and AGE-BSA-dependent AP-1 activity on electrophoretic mobility shift assay (Fig. 5A) and the VEGF expression on Northern blots (Fig. 5B).

Effect of MAPK inhibitor

Next, we studied the effects of a specific inhibitor of ERK1/2, PD98059 [2-(2′-amino-3′-methylphenyl) oxanaphthalene-4-one], on the AGE-induced activation of ERK1/2 and the expression of VEGF mRNA. The AGE-stimulated activity of ERK1/2 was abolished by PD98059 (Fig. 5C). PD98059 also inhibited the expression of VEGF mRNA (Fig. 5D) induced by AGEs.

Estimation of ROS

Production of ROS by AGEs was estimated by flow cytometric analysis using DCFH-DA as a substrate. Figure 6A shows the production of ROS in RAW264.7 cells treated with AGEs for 3 h. RAW264.7 cells were treated with 50 μg/ml and 100 μg/ml of CML-BSA, and 100 μg/ml and 200 μg/ml of AGE-BSA. ROS was produced in the cells dependent on the concentration of AGE-BSA ($^{*}p < .05$ vs. control). Production of ROS by CML-BSA was not significant, even though the production seemed dose-dependent. The production of ROS by AGE-BSA

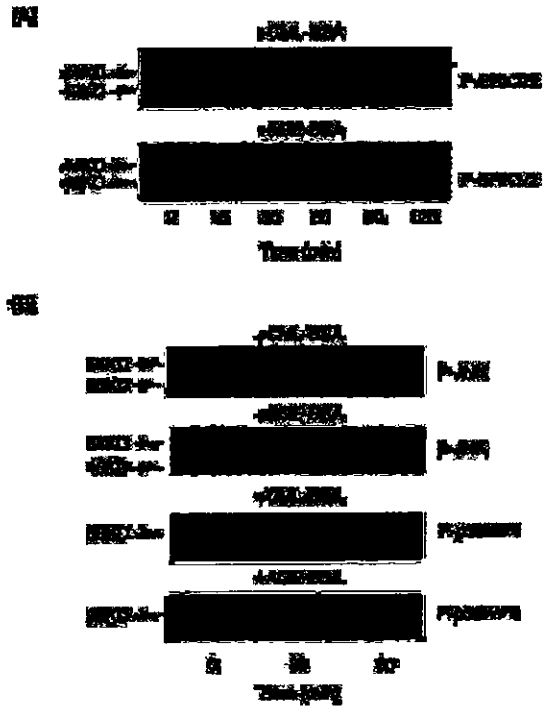

Fig. 4. MAPK assay. Phosphorylation of ERK1/2 (P-ERK1/2) (A), JNK (P-JNK), and $p38^{MAPK}$ (P- $p38^{MAPK}$) (B) after the treatment of cells with 100 μg/ml of CML-BSA or 200 μg/ml of AGE-BSA was measured at the indicated incubation times by Western blot analysis. The cells were rinsed twice with ice-cold phosphate-buffered saline, and lysed in buffer containing 20 mM HEPES (pH 7.4), 50 mM glycerophosphate, 1% Triton X-100, 10% glycerol, 2 mM EGTA, 1 mM DTT, 10 mM sodium fluoride, 1 mM sodium orthovanadate, 2 μM leupeptin, 2 μM aprotinin, 2 μM pepstatin A, and 1 mM PMSF. Soluble extracts were prepared by centrifugation at 10,000 × *g* for 10 min at 4°C. Proteins (25 μg) were separated on 10% polyacrylamide gels using SDS-PAGE and transferred to Hybond-ECL nitrocellulose membranes. Membranes were incubated for 1 h with primary antibodies. After incubation with secondary antibodies for 1 h, phosphorylated forms of protein were detected by ECL chemiluminescence.

continued for over 6 h, whereas it was not observed by CML-BSA (data not shown).

Effect of antioxidants

Figure 6B shows the effect of antioxidants on the production of ROS by AGEs. RAW264.7 cells were previously treated with 0.5 mM Trolox, a synthetic vitamin E, for 1 h (lanes 3 and 4), with 5 mM NAC for 6 h (lanes 5 and 6), or with AGE-BSA pretreated with 50 mM $NaBH_4$ for 1 h, to reduce reactive intermediates (lane 7 and 8). These treatments decreased the AGE-BSA-induced production of ROS. N-acetyl cysteine (NAC) inhibited the AGE-BSA-induced production of ROS by 46%. Trolox inhibited the production of ROS in AGE-BSA-treated cells by 66%, while $NaBH_4$ decreased it by 83%. An inhibitory effect of NAC was also observed on the CML-BSA-induced production of ROS only 5% inhibition, however, Trolox and $NaBH_4$ had no effect (data not shown). As described above, there was a difference in the duration of the stimulation of intracellular signal pathways between AGE-BSA and CML-BSA. To elucidate whether ROS plays a role in the AGE-BSA-induced VEGF expression, and relationship

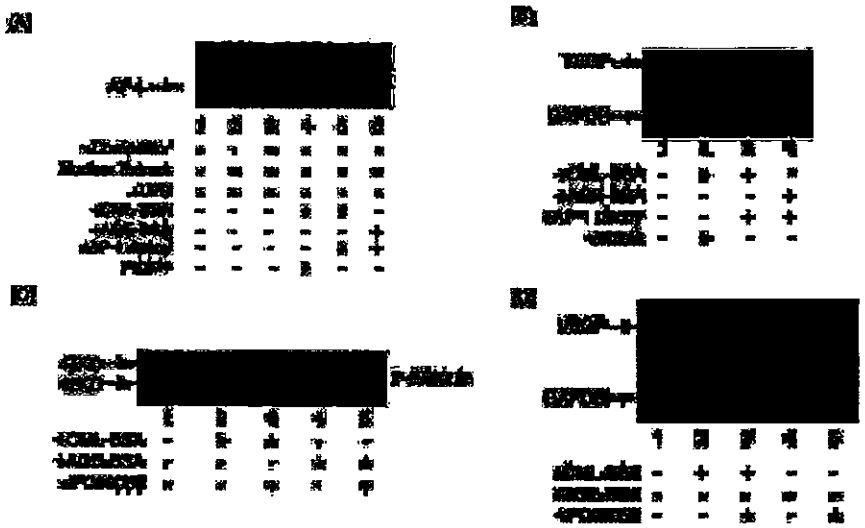

Fig. 5. Decoy approach and effect of ERK1/2 inhibitor. To affirm the role of AP-1 in the induction of VEGF by CML-BSA, an AP-1 decoy approach was adopted. *Cis*-element double-stranded oligodeoxynucleotide was synthesized using 5'-CCGCCACTGACTA-ACTCCAG-3' and 3'-GGCGGTGACTGATTGAGGTC-5'. RAW264.7 cells were exposed to an AP-1 decoy or vehicle (control). One day before transfection, cells were seeded at a density of 1×10^6 cells/well in to six-well plates. Three micromolar decoy oligonucleotides were added 24 h before the treatment with AGEs. (A) Electrophoretic mobility shift assay of AP-1 and (B) Northern blots of VEGF, 1 h for CML-BSA and 5 h for AGE-BSA after the addition of AGEs, respectively. Second, the effect of a specific inhibitor of MEK1, PD98059 [2-(2'-amino-3'-methylphenyl)oxanaphthalene-4-one], on the AP-1-DNA binding activity and the expression of VEGF mRNA stimulated by AGEs was evaluated. RAW264.7 cells were incubated with 50 μM PD98059 for 1 h then treated with 100 μg/ml of CML-BSA for 6 h or 200 μg/ml of AGE-BSA for 9 h. (C) The phosphorylation of ERK1/2 (P-ERK1/2) on Western blots; (D) The expression of VEGF mRNA on Northern blots.

between the production of ROS and induction of VEGF by AGEs, AGE-BSA was pretreated with 50 mM $NaBH_4$ for 1 h ($NaBH_4$-treated AGE-BSA). Figure 7 shows the effect of $NaBH_4$-treated AGE-BSA on the activity of ERK1/2 (A), the activity of Raf-1 kinase (B), and the expression of VEGF mRNA (C). $NaBH_4$-treated AGE-BSA decreased the phosphorylation of ERK1/2 mediated by AGE-BSA. Notably, the phosphorylation observed at 90 and 120 min in the AGE-BSA-treated cells was abolished by reduction with $NaBH_4$. Concomitantly, the activity of Raf-1 kinase and the expression of VEGF were suppressed by $NaBH_4$-treated AGE-BSA. Decrease in the expression of VEGF was also observed in the cells incubated with $NaBH_4$-treated AGE-BSA (C).

DISCUSSION

In diabetic complications such as retinopathy and renopathy, VEGF is a major growth factor that has an adverse effect on pathological angiogenesis. Therapeutic approaches using VEGF inhibitors to prevent these diabetic complications have been investigated [18,43,44]. Since an accumulation of AGEs, especially CML adducts, has been found in tissues from DM in which neovascularization was observed [5–9], we speculated on a possible role for AGE adducts in the progression of diabetic angiopathy. In the present study, we examined whether AGE adducts induce the production of angiogenic growth factors, and if so, the mechanism by which angiogenesis is induced by these adducts. The following evidence was obtained: (i) Both CML-BSA and AGE-BSA stimulated the expression of VEGF and ANG mRNAs in mouse macrophage like RAW264.7 cells. (ii) The induction of VEGF by AGEs was mediated by AP-1. The effect of AGE-BSA on the AP-1 activity mediated by Ras/Raf-1/ERK1/2 signal pathways lasted longer than that of CML-BSA and was concomitant with the production of ROS. (iii) ROS-dependent induction of VEGF

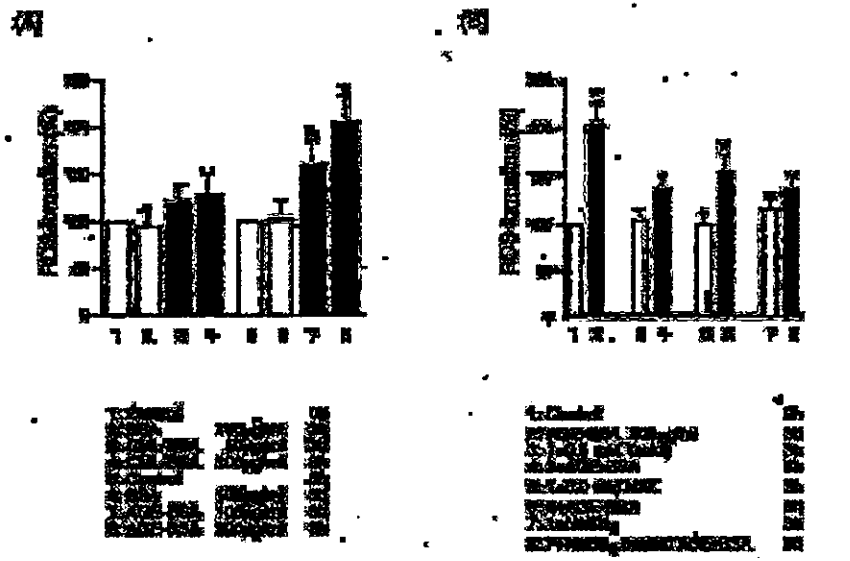

Fig. 6. Estimation of ROS. Production of ROS in RAW264.7 cells treated with AGEs was estimated by flow cytometric analysis using DCFH-DA as a substrate. (A) RAW264.7 cells were treated with 50 μg/ml and 100 μg/ml of CML-BSA, and 100 μg/ml and 200 μg/ml of AGE-BSA for 3 h. *$p < 0.05$ vs lane 5. (B) Effect of antioxidants on the AGE-induced ROS production was determined. RAW264.7 cells were previously treated with 5 mM NAC for 6 h or 0.5 mM Trolox for 1 h. In order to reduce reactive intermediates, AGE-BSA was previously treated with 50 mM $NaBH_4$ for 1 h. The equal volume of 50 mM $NaBH_4$ was added to medium as a control (lane 7). The intensity was expressed as a percentage of the control. Statistical difference was analyzed using one-way Fractional ANOVA test. *$p < .0001$ vs. lane 1. Data are the mean ± SD (%) of three independent analyses.

was abolished by antioxidants or the reduction of AGE-BSA. However, the mechanism of induction of ANG mRNA by AGEs is unclear.

Macrophages remove AGE-modified proteins through cell surface RAGEs [4,10,12]. In addition to the uptake and degradation of AGEs, interactions between AGE-legends and RAGEs induce a range of biologically important responses by macrophages, including chemotaxis [45], cellular activation, and the secretion of cytokines and growth factors [46–48]. For example, AGEs induce the production of TNF-α, interleukin-1, platelet-derived growth factor, and insulin-like growth factor-1 in macrophages [46]. AGEs also induce the expression of VCAM-1, an adhesion molecule, in endothelial cells [49].

Kislinger et al. has reported a role for CML in intracellular signaling pathways and the modulation of gene expression [4]. One pathway of RAGE-dependent cellular perturbation involves the activation of $p21^{ras}$, followed by the activation of NF-κB, resulting in the transcription of target genes [27,49,50]. In the present study, the AP-1-DNA binding activity (Fig. 2), the CAT activity for the VEGF promoter (Fig. 3), and abrogation of the AGE-induced VEGF expression using an AP-1 decoy (Fig. 5), suggested that AGEs upregulate the VEGF expression mediated by AP-1. Activation of MAPK signaling pathways by AGEs was observed (Fig. 4). In RAW264.7 cells, AGEs stimulated NF-κB, however, a NF-κB decoy approach showed that the induction of VEGF by AGEs was independent of NF-κB activity (data not shown).

The intracellular formation of AGEs may reflect intracellular oxidative stress [26]. On the other hand, ROS is induced by AGEs and has been implicated in the activation of AP-1 [51]. Similarly, Yan et al. reported that oxidative stress is involved in RAGE-induced cellular activation [27]. It is therefore speculated that ROS plays a role in the CML-adducts/RAGE-mediated signal cascade. Flow cytometric analysis revealed production of ROS by AGEs (Fig. 6). AGE-BSA produced more intracellular ROS than CML-BSA. There may be direct and indirect mechanisms for the production of ROS by

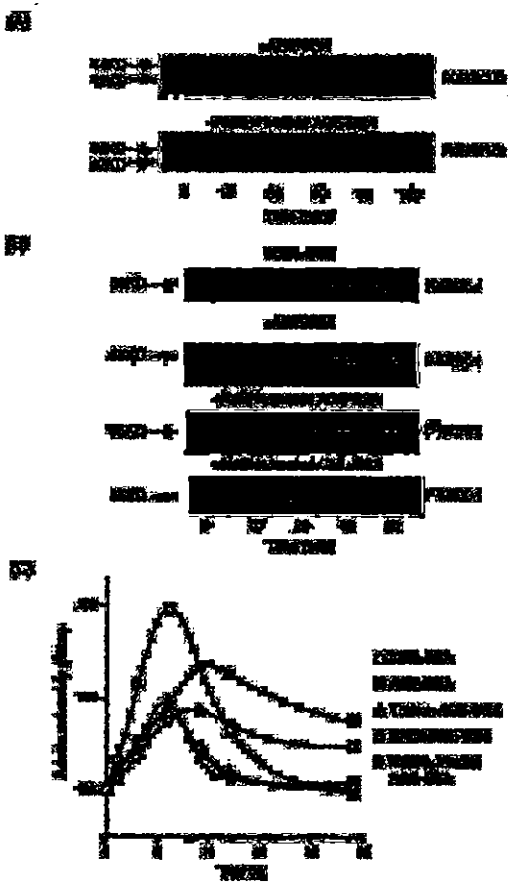

Fig. 7. Effect of attenuation of ROS. The effect of attenuation of ROS on AGE-stimulated the phosphorylation of ERK1/2 (A), Raf-1 kinase activity (B), and VEGF mRNA expression (C) was estimated. (A) RAW264.7 cells were incubated with 200 μg/ml of AGE-BSA with or without pretreatment with 50 mM $NaBH_4$ for 1 h. (B) RAW264.7 cells were treated with 100 μg/ml of CML-BSA, or 200 μg/ml of AGE-BSA with or without pretreatment with 50 mM $NaBH_4$ for 1 h. ^{32}P labeled MEK-1 (p-MEK-1) was analyzed using BAS5000. (C) RAW264.7 cells were incubated with 100 μg/ml of CML-BSA (□), or 200 μg/ml of AGE-BSA (■) with or without the treatment with NAC (○) and Trolox (△), or 200 μg/ml of $NaBH_4$ treated AGE-BSA (●).

AGEs: direct formation in the cell surface membranes [2] and indirect formation mediated by Ras or NADPH oxidase during activation of the intracellular signaling pathways [29]. It has been reported that NADPH oxidase is activated by AGEs [52]. The activation of NADPH oxidase and production of ROS by AGEs were observed after 16 h incubation. In our study, production of ROS was observed within a few hours (Fig. 6) and was not inhibited by DPI, a specific inhibitor of NADPH oxidase. And AGEs did not alter the levels of GSH nor the activity of total SOD after 12 h incubation (data not shown). The precise mechanisms by which ROS is produced were not clarified, however, it seems likely that ROS produced by AGE-BSA is generated in the cell surface membranes independent from receptor-mediated signals [2] or decrease in the intracellular antioxidants, and lesser amounts of ROS are produced in CML-BSA-treated cells through intracellular signaling pathways, such as Ras/Raf-1 activity [53].

It is known that the activity of AP-1 is modulated by redox potential [54]. The DNA-binding of AP-1 is modulated by redox. Abate et al. found that reduction of a single cystine in the DNA-binding domain of c-Jun and c-Fos is necessary for the DNA-binding of the Fos/Jun heterodimer [55]. In the present study, pretreatment of RAW264.7 cells with NAC, a thiol-containing antioxidant and a precursor of GSH, and Trolox resulted in an inhibition of ROS production (Fig. 6) and the VEGF mRNA expression induced by AGEs (Fig. 7). $NaBH_4$-treated AGE-BSA lost the production of ROS (Fig. 6B) and duration of the induction of VEGF (Fig. 7C). The data suggest that the induction of VEGF by AGEs is receptor-mediated signals and it is further stimulated by ROS produced by AGE-BSA. Even though the regulation of the activity of MAPKs and AP-1 is complex [54] and the precise mechanism was not studied, the data in the present study support the idea that ROS participates in AGE-BSA-induced expression of VEGF mediated by the activities of Ras/Raf/MEK/ERK1/2, and the AP-1-DNA binding activity. The induction of VEGF mRNA by AGE-BSA was partially inhibited by antioxidants (Fig. 7).

In diabetic patients, AGEs directly alter extracellular protein through glycation-induced cross-link formation and affect the interaction between endothelial cells and the extracellular matrix, resulting in the impairment of neovascularization [56]. The production of VEGF and ANG induced by AGEs may correlate with the capacity of macrophages to promote neovascularization and enhance vascular permeability in diabetic microangiopathy in retina or kidney. However, coronary collateral development and neovascularization are inhibited in diabetic conditions [57], suggesting presence of difference of the expression of VEGF by different signal activities in different tissues. In conclusion, AGEs induce the expression of VEGF mRNA mediated by AP-1 in macrophages to affect endothelial cell mitogenesis and vascular permeability. A therapeutic strategy for scavenging ROS in the AGE-mediated progression of diabetic complications was also suggested.

Acknowledgements — This work was supported by a grant-in-aid for Scientific Research (10470041) from the Ministry of Education, Sports and Culture of Japan. The authors thank Ms. J. Tagaya for technical assistance, and Dr. H. A. Weich (Department of Gene Regulation and Differentiation, National Center for Biotechnology, Branschweig, Germany) for kindly providing VEGF cDNA.

REFERENCES

[1] Ahmed, M. U.; Thorpe, S. R.; Baynes, J. W. Identification of N^{ε}-(carboxymethyl-)lysine as a degradation product of fructose-lysine in glycated proteins. *J. Biol. Chem.* **261**:4889–4898; 1986.
[2] Taniguchi, N.; Kaneto, H.; Asahi, M.; Takahashi, M.; Wenyi, C.; Higashiyama, S.; Fujii, J.; Suzuki, K.; Kayanoki, Y. Involvement of glycation and oxidative stress in diabetic macroangiopathy. *Diabetes* **45**:S81–S83; 1996.
[3] Nagai, R.; Ikeda, K.; Higashi, T.; Sano, H.; Jinnouchi, Y.; Araki, T.; Horiuchi, S. Hydroxyl radical mediates N epsilon-(carboxymethyl)lysine formation from amadori product. *Biochem. Biophys. Res. Commun.* **234**:167–172; 1997.
[4] Kislinger, T.; Fu, C.; Huber, B.; Qu, W.; Taguchi, A.; Yan, S. D.; Hofmann, M.; Yan, S. F.; Pischetsrieder, M.; Stern, D.; Schmidt, A. M. N(epsilon)-(carboxymethyl)lysine adducts of proteins are ligands for receptor for advanced glycation end products that activate cell signaling pathways and modulate gene expression. *J. Biol. Chem.* **274**:31740–31749; 1999.
[5] Schleicher, E. D.; Wagner, E.; Nerlich, A. G. Increased accumulation of the glycoxidation product N(epsilon)-(carboxymethyl)-lysine in human tissues in diabetes and aging. *J. Clin. Invest.* **99**:457–468; 1997.
[6] Berg, T. J.; Clausen, J. T.; Torjesen, P. A.; Dahl-Jorgensen, K.; Bangstad, H. J.; Hanssen, K. F. The advanced glycation end product Nepsilon-(carboxymethyl)lysine is increased in serum from children and adolescents with type 1 diabetes. *Diabetes Care* **21**:1997–2002; 1998.
[7] Sakata, N.; Imanaga, Y.; Meng, J.; Tachikawa, Y.; Takebayashi, S.; Nagai, R.; Horiuchi, S. Increased advanced glycation end products in atherosclerotic lesions of patients with end-stage renal disease. *Atherosclerosis* **142**:67–77; 1999.
[8] Miyata, T.; Ishikawa, S.; Asahi, K.; Inagi, R.; Suzuki, D.; Horie, K.; Tatsumi, K.; Kurokawa, K. 2-Isopropylidenehydrazono-4-oxo-thiazolidin-5-ylacetanilide (OPB-9195) treatment inhibits the development of intimal thickening after balloon injury of rat carotid artery: role of glycoxidation and lipoxidation reactions in vascular tissue damage. *FEBS Lett.* **445**:202–206; 1999.
[9] Horie, K.; Miyata, T.; Maeda, K.; Miyata, S.; Sugiyama, S.; Sakai, H.; van Strihou, C. Y.; Monnier, V. M.; Witztum, J. L.; Kurokawa, K. Immunohistochemical colocalization of glycoxidation products and lipid peroxidation products in diabetic renal glomerular lesions. Implication for glycoxidative stress in the pathogenesis of diabetic nephropathy. *J. Clin. Invest.* **100**:2995–3004; 1997.
[10] Radoff, S.; Cerami, A.; Vlassara, H. Isolation of surface binding protein specific for advanced glycosylation end products from mouse macrophage-derived cell line RAW 264.7. *Diabetes* **39**:1510–1518; 1990.
[11] Nachtigal, M.; AL-Assaad, Z.; Mayer, E. P.; Kim, K.; Monsigny, M. Galectin-3 expression in human atherosclerotic lesions. *Am. J. Pathol.* **152**:1199–1208; 1998.
[12] Radoff, S.; Vlassara, H.; Cerami, A. Characterization of a solubilized cell surface binding protein on macrophages specific for proteins modified nonenzymatically by advanced glycosylated end products. *Arch. Biochem. Biophys.* **263**:418–423; 1988.
[13] Gospodarowicz, D.; Abraham, J. A.; Schilling, J. Isolation and characterization of a vascular endothelial cell mitogen produced by pituitary-derived folliculo stellate cells. *Proc. Natl. Acad. Sci. USA* **86**:7311–7315; 1989.
[14] Ferrara, N.; Henzel, W. J. Pituitary follicular cells secrete a novel heparin-binding growth factor specific for vascular endothelial cells. *Biochem. Biophys. Res. Commun.* **161**:851–858; 1989.
[15] Tischer, E.; Mitchell, R.; Hartman, T.; Silva, M.; Gospodarowicz, D.; Fiddes, J. C.; Abraham, J. A. The human gene for vascular endothelial growth factor. Multiple protein forms are encoded through alternative exon splicing. *J. Biol. Chem.* **266**:11947–11954; 1991.
[16] Shweiki, D.; Itin, A.; Soffer, D.; Keshet, E. Vascular endothelial growth factor induced by hypoxia may mediate hypoxia-initiated angiogenesis. *Nature* **359**:843–845; 1992.
[17] Samoto, K.; Ikezaki, K.; Ono, M.; Shono, T.; Kohno, K.; Ku-

wano, M.; Fukui, M. Expression of vascular endothelial growth factor and its possible relation with neovascularization in human brain tumors. *Cancer Res.* 55:1189–1193; 1995.
[18] Tsuchida, K.; Makita, Z.; Yamagishi, S.; Atsumi, T.; Miyoshi, H.; Obara, S.; Ishida, M.; Ishikawa, S.; Yasumura, K.; Koike, T. Suppression of transforming growth factor beta and vascular endothelial growth factor in diabetic nephropathy in rats by a novel advanced glycation end product inhibitor, OPB-9195. *Diabetologia* 42:579–588; 1999.
[19] Ryuto, M.; Ono, M.; Izumi, H.; Yoshida, S.; Weich, H. A.; Kohno, K.; Kuwano, M. Induction of vascular endothelial growth factor by tumor necrosis factor alpha in human glioma cells. Possible roles of SP-1. *J. Biol. Chem.* 271:28220–28228; 1996.
[20] Yeh, C. H.; Sturgis, L.; Haidacher, J.; Zhang, X. N.; Sherwood, S. J.; Bjercke, R. J.; Juhasz, O.; Crow, M. T.; Tilton, R. G.; Denner, L. Requirement for p38 and p44/p42 mitogen-activated protein kinases in RAGE-mediated nuclear factor-kappaB transcriptional activation and cytokine secretion. *Diabetes* 50:1495–1504; 2001.
[21] Miura, T.; Nagai, R.; Ishibashi, T.; Inomuta, H.; Ikeda, K.; Horiuchi, S. The relationship between accumulation of advanced glycation end products and expression of vascular endothelial growth factor in human diabetic retinas. *Diabetologia* 40:764–769; 1997.
[22] Fett, J. W.; Strydom, D. J.; Lobb, R. R.; Alderman, E. M.; Bethune, J. L.; Riordan, J. F.; Vallee, B. L. Isolation and characterization of angiogenin, an angiogenic protein from human carcinoma cells. *Biochemistry* 24:5480–5486; 1985.
[23] Gho, Y. S.; Chae, C. B. Anti-angiogenin activity of the peptides complementary to the receptor-binding site of angiogenin. *J. Biol. Chem.* 272:24294–24299; 1997.
[24] Malamitsi-Puchner, A.; Sarandakou, A.; Dafogianni, C.; Tziotis, J.; Bartsocas, C. S. Serum angiogenin levels in children and adolescents with insulin-dependent diabetes mellitus. *Pediatr. Res.* 43:798–800; 1998.
[25] Ozaki, H.; Hayashi, H.; Oshima, K. Angiogenin levels in the vitreous from patients with proliferative diabetic retinopathy. *Ophthalmic Res.* 28:356–360; 1996.
[26] Hammes, H. P.; Brownlee, M.; Lin, J.; Schleicher, E.; Bretzel, R. G. Diabetic retinopathy risk correlates with intracellular concentrations of the glycoxidation product Nepsilon-(carboxymethyl) lysine independently of glycohaemoglobin concentrations. *Diabetologia* 42:603–607; 1999.
[27] Yan, S. D.; Schmidt, A. M.; Anderson, G. M.; Zhang, J.; Brett, J.; Zou, Y. S.; Pinsky, D.; Stern, D. Enhanced cellular oxidant stress by the interaction of advanced glycation end products with their receptors/binding proteins. *J. Biol. Chem.* 269:9889–9897; 1994.
[28] Dong, C.; Goldschmidt-Clermont, P. J. Ras activation of NF-kappa B and superoxide. *Methods Enzymol.* 333:88–96; 2001.
[29] Thannickal, V. J.; Day, R. M.; Klinz, S. G.; Bastien, M. C.; Larios, J. M.; Fanburg, B. L. Ras-dependent and -independent regulation of reactive oxygen species by mitogenic growth factors and TGF-β1. *FASEB J.* 14:1741–1748; 2000.
[30] Shih, N.-L.; Cheng, T.-H.; Loh, S.-H.; Cheng, P.-Y.; Wang, D. L.; Chen, Y.-S.; Liu, S.-H.; Liew, C.-C.; Chen, J.-J. Reactive oxygen species modulate angiotensin II-induced β-myosin heavy chain gene expression via ras/raf/extracellular signal-regulated kinase pathway in neonatal rat cardiomyocytes. *Biochem. Biophys. Res. Commun.* 283:143–148; 2001.
[31] Weindel, K.; Marme, D.; Weich, H. A. AIDS-associated Kaposi's sarcoma cells in culture express vascular endothelial growth factor. *Biochem. Biophys. Res. Commun.* 183:1167–1174; 1992.
[32] Takata, K.; Horiuchi, S.; Araki, N.; Shiga, M.; Saitoh, M.; Saitoh, M.; Morino, Y. Endocytic uptake of nonenzymatically glycosylated proteins is mediated by a scavenger receptor for aldehyde-modified proteins. *J. Biol. Chem.* 263:14819–14825; 1988.
[33] Chibber, R.; Molinatti, P. A.; Kohner, E. M. Intracellular protein glycation in cultured retinal capillary pericyte endothelial cells exposed to high-glucose concentration. *Cell. Mol. Biol. (Noisy-le-grand)* 45:47–57; 1999.
[34] Godwin, A. K.; Meister, A.; O'Dwyer, P. J.; Huang, C. S.; Hamilton, T. C.; Anderson, M. E. High resistance to cisplatin in human ovarian cancer cell lines is associated with marked increase of glutathione synthesis. *Proc. Natl. Acad. Sci. USA* 89:3070–3074; 1992.
[35] Sambrook, J.; Fritsch, E. F.; Maniatis, T. Analysis of RNA. In: Sambrook, J.; et al., eds. *Molecular cloning: a laboratory manual*, 2nd ed. Cold Spring Harbor, NY: Cold Spring Harbor Laboratory Press; 1989:7–39.
[36] Abmayr, S. M.; Workman, J. L. Mobility shift DNA-binding assay using gel electrophoresis. In: Ausubel, F. M.; Brent, R.; et al., eds. *Current protocols in molecular biology*, vol. 11. New York: Greene Publishing Associates and Wiley-Interscience; 1987:1203–1219.
[37] Sen, R.; Baltimore, D. Multiple nuclear factors interact with the immunoglobulin enhancer sequences. *Cell* 46:705–716; 1986.
[38] von Knethen, A.; Callsen, D.; Brüne, B. Superoxide attenuates macrophage apoptosis by NF-kappa B and AP-1 activation that promotes cyclooxygenase-2 expression. *J. Immunol.* 163:2858–2866; 1999.
[39] Kubo, T.; Kohno, K.; Ohga, T.; Taniguchi, K.; Kawanami, K.; Wada, M.; Kuwano, M. DNA topoisomerase II alpha gene expression under transcriptional control in etoposide/teniposide-resistant human cancer cells. *Cancer Res.* 55:3860–3864; 1995.
[40] Rosenthal, N. Identification of regulatory elements of cloned genes with functional assays. *Methods Enzymol.* 152:704–720; 1987.
[41] Egea, J.; Espinet, C.; Comella, J. X. Calcium influx activates extracellular-regulated kinase/mitogen-activated protein kinase pathway through a calmodulin-sensitive mechanism in PC12 cells. *J. Biol. Chem.* 274:75–85; 1999.
[42] Bass, D. A.; Parce, J. W.; Dechatelet, L. R.; Szejda, P.; Seeds, M. C.; Thomas, M. Flow cytometric studies of oxidative product formation by neutrophils: an oxidative response to membrane stimulation. *J. Immunol.* 130:1910–1917; 1983.
[43] Spranger, J.; Hammes, H. P.; Preissner, K. T.; Schatz, H.; Pfeiffer, A. F. Release of the angiogenesis inhibitor angiostatin in patients with proliferative diabetic retinopathy: association with retinal photocoagulation. *Diabetologia* 43:1404–1407; 2000.
[44] Gilbert, R. E.; Kelly, D. J.; Cox, A. J.; Wilkinson-Berka, J. L.; Rumble, J. R.; Osicka, T.; Panagiotopoulos, S.; Lee, V.; Hendrich, E. C.; Jerums, G.; Cooper, M. E. Angiotensin converting enzyme inhibition reduces retinal overexpression of vascular endothelial growth factor and hyperpermeability in experimental diabetes. *Diabetologia* 43:1360–1367; 2000.
[45] Higashi, T.; Sano, H.; Saishoji, T.; Ikeda, K.; Jinnouchi, Y.; Kanzaki, T.; Morisaki, N.; Rauvala, H.; Shichiri, M.; Horiuchi, S. The receptor for advanced glycation end products mediates the chemotaxis of rabbit smooth muscle cells. *Diabetes* 46:463–472; 1997.
[46] Pugliese, G.; Pricci, F.; Romeo, G.; Pugliese, F.; Mene, P.; Giannini, S.; Cresci, B.; Galli, G.; Rotella, C. M.; Vlassara, H.; Mario, U. Upregulation of mesangial growth factor and extracellular matrix synthesis by advanced glycation end products via a receptor-mediated mechanism. *Diabetes* 46:1881–1887; 1997.
[47] Vlassara, H.; Brownlee, M.; Manogue, K. R.; Dinarello, C. A.; Pasagian, A. Cachectin/TNF and IL-1 induced by glucose-modified proteins: role in normal tissue remodeling. *Science* 240:1546–1548; 1988.
[48] Kirstein, M.; Aston, C.; Hintz, R.; Vlassara, H. Receptor-specific induction of insulin-like growth factor I in human monocytes by advanced glycosylation end product-modified proteins. *J. Clin. Invest.* 90:439–446; 1992.
[49] Schmidt, A. M.; Hori, O.; Chen, J.-X.; Li, J.-F.; Crandall, J.; Zhang, J.; Cao, R.; Yan, S. D.; Brett, J.; Stern, D. Advanced glycation endproducts interacting with their endothelial receptor induce expression of vascular cell adhesion molecule-1 (VCAM-1) in cultured human endothelial cells and in mice. A potential mechanism for the accelerated vasculopathy of diabetes. *J. Clin. Invest.* 96:1395–1403; 1995.
[50] Lander, H. M.; Tauras, J. M.; Ogiste, J. S.; Hori, O.; Moss, R. A.; Schmidt, A. M. Activation of the receptor for advanced glycation

end products triggers a p21(ras)-dependent mitogen-activated protein kinase pathway regulated by oxidant stress. *J. Biol. Chem.* 272:17810–17814; 1997.
[51] Simm, A.; Mönch, G.; Seif, F.; Schenk, O.; Heidland, A.; Richter, H.; Vamvakas, S.; Schinzel, R. Advanced glycation endproducts stimulate the MAP-kinase pathway in tubulus cell line LLC-PK1. *FEBS Lett.* 410:481–484; 1997.
[52] Wautier, M.-P.; Chappey, O.; Corda, S.; Stern, D. M.; Schmidt, A. M.; Wautier, J.-L. Activation of NADPH oxidase by AGE links oxidant stress to altered gene expression via RAGE. *Am. J. Physiol. Endocrinol. Metab.* 280:E685–E694; 2001.
[53] Griendling, K. K.; Sorescu, D.; Lassegue, B.; Ushio-Fukai, M. Modulation of protein kinase activity and gene expression by reactive oxygen species and their role in vascular physiology and pathophysiology. *Arterioscler Thromb. Vasc. Biol.* 20:2175–2183; 2000.
[54] Arrigo, A. P.; Kretz-Remy, C. Regulation of mammalian gene expression by free radicals. In: Aruoma, O. I.; Halliwell, B., eds. *Molecular biology of free radicals in human diseases*. Saint Lucia, London: Oica International; 1998:183–223.
[55] Abate, C.; Patel, L.; Rauscher, F. J. III; Curran, T. Redox regulation of fos and jun DNA-binding activity in vitro. *Science* 249:1157–1161; 1990.
[56] Kuzuya, M.; Satake, S.; Ai, S.; Asai, T.; Kanda, S.; Ramos, M. A.; Miura, H.; Ueda, M.; Iguchi, A. Inhibition of angiogenesis on glycated collagen lattices. *Diabetologia* 41:491–499; 1998.
[57] Rivard, A.; Silver, M.; Chen, D.; Kearney, M.; Magner, M.; Annex, B.; Peters, K.; Isner, J. M. Rescue of diabetes-related impairment of angiogenesis by intramuscular gene therapy with adeno-VEGF. *Am. J. Pathol.* 154:355–363; 1999.

ABBREVIATIONS

AGE—advanced glycation end product
ANG—angiogenin
AP-1—activator protein-1
bFGF—basic fibroblast growth factor
BSA—bovine serum albumin
CML—N(epsilon)-(carboxymethyl)lysine
GSH—glutathione
GAPDH—glyceraldehyde-3-phosphate dehydrogenase
MAPK—mitogen-activated protein kinase
ERK1/2—the extracellular signal-regulated kinases 1 and 2
NAC—N-acetylcysteine
NF-κB—nuclear factor-κB
PSL—photostimulated luminescence
Sp1—specificity protein-1
VEGF—vascular endothelial growth factor

ELSEVIER

EXPERIMENTAL HEMATOLOGY

Experimental Hematology 32 (2004) 375–381

Ascorbic acid restores sensitivity to imatinib via suppression of Nrf2-dependent gene expression in the imatinib-resistant cell line

Takahisa Tarumoto[a], Tadashi Nagai[a], Ken Ohmine[a], Takuji Miyoshi[a], Makiko Nakamura[a], Takahito Kondo[b], Kenji Mitsugi[c], Syuji Nakano[c], Kazuo Muroi[d], Norio Komatsu[a], and Keiya Ozawa[a]

Divisions of [a]Hematology and [d]Cell Transplantation and Transfusion, Jichi Medical School, Tochigi, Japan; [b]Department of Biochemistry and molecular Biology in Disease, Atomic Bomb Disease Institute, Nagasaki University Graduate School of Medicine, Nagasaki, Japan; [c]First Department of Internal Medicine, Faculty of Medicine, Kyushu University, Fukuoka, Japan

(Received 11 August 2003; revised 1 December 2003; accepted 15 January 2004)

Objective. **Imatinib, a BCR/ABL tyrosine kinase inhibitor, has shown remarkable clinical effects in chronic myelogenous leukemia. However, the leukemia cells become resistant to this drug in most blast crisis cases. The transcription factor Nrf2 regulates the gene expression of a number of detoxifying enzymes such as γ-glutamylcysteine synthetase (γ-GCS), the rate-limiting enzyme in glutathione (GSH) synthesis, via the antioxidant response element (ARE). In this study, we examined the involvement of Nrf2 in the acquisition of resistance to imatinib. Since oxidative stress promotes the translocation of Nrf2 from the cytoplasm to the nucleus, we also examined whether ascorbic acid, a reducing reagent, can overcome the resistance to imatinib by inhibiting Nrf2 activity.**

Results. **Binding of Nrf2 to the ARE of the γ-GCS light subunit (γ-GCSl) gene promoter was much stronger in the imatinib-resistant cell line KCL22/SR than in the parental imatinib-sensitive cell line KCL22. The levels of γ-GCSl mRNA and GSH were higher in KCL22/SR cells, a finding consistent with the observation of an increase in Nrf2-DNA binding. Addition of a GSH monoester to KCL22 cells resulted in an increase in the IC_{50} value of imatinib. In contrast, addition of ascorbic acid to KCL22/SR cells resulted in a decrease in Nrf2-DNA binding and decreases in levels of γ-GCSl mRNA and GSH. Consistent with these findings, ascorbic acid partly restored imatinib sensitivity to KCL22/SR.**

Conclusion. **Changes in the redox state caused by antioxidants such as ascorbic acid can overcome resistance to imatinib via inhibition of Nrf2-mediated gene expression.** © 2004 **International Society for Experimental Hematology. Published by Elsevier Inc.**

Imatinib (imatinib mesylate: Novartis Pharmaceuticals, Basel, Switzerland), a specific BCR/ABL tyrosine kinase inhibitor, has been shown to be effective for treatment of chronic myelogenous leukemia (CML) in blast crisis (BC) and in chronic phase (CP) [1–2]. In recent clinical studies of imatinib with large numbers of BC patients, around 50% of patients achieved hematologic response [3]. However, drug resistance is a major problem for imatinib treatment of CML patients in BC because substantial numbers of patients have relapsed relatively soon after treatment with imatinib [2,3]. Previous studies have demonstrated possible mechanisms involved in resistance to imatinib. These include amplification of and mutations in the BCR/ABL gene, increased expression of BCR/ABL protein and p-glycoprotein, and an increase in serum α1 acid glycoprotein [4–9]. However, some imatinib-resistant cells show none of these changes [6], suggesting that the mechanisms involved in resistance to imatinib are very complex.

Nrf2, a member of the CNC family of basic region-leucine zipper transcription factors, has been shown to bind to antioxidant-responsive element (ARE) [10,11]. ARE has been found in the promoter region of several detoxifying and antioxidative stress genes such as γ-glutamylcystein synthetase (γ-GCS) and glutathione-S-transferase (GST). Nrf2 contains 6 conserved domains: Neh1 to Neh6. Previous analysis has shown that Keap1, a homologue of the Drosophila actin-binding protein Kelch, binds to the Neh2 domain of Nrf2

Offprint requests to: Tadashi Nagai, M.D., Ph.D., Jichi Medical School, 3311-1 Yakushiji, Minamikawachi-machi, Kawachi-gun, Tochigi 329-0498, Japan; E-mail: t-nagai@jichi.ac.jp

doi: 10.1016/j.exphem.2004.01.007

in cytoplasm in a "nonstimulated"condition [12]. Activation inducers for Nrf2 such as oxidative stress cause dissociation of these two factors, resulting in migration of Nrf2 into the nucleus. There, Nrf2 binds to ARE as a heterodimer with other transcription factors, such as small Maf family proteins, and regulates ARE-mediated gene expression. Because induction of phase II detoxifying enzymes is significantly reduced in Nrf2 knockout mice and induction of some antioxidative stress genes such as hemeoxygenase I is severely impaired in Nrf2-deficient macrophages [13,14], it is thought that Nrf2 is necessary for expression of antioxidative stress genes as well as phase II detoxifying enzymes.

γ-GCS, the rate-limiting enzyme of the glutathione (GSH) synthetic pathway, catalyzes condensation of L-glutamate and L-cystein, to form L-γ-glutamylcysteine [15]. GSH, a prominent cellular nonprotein thiol, functions as a cellular antioxidant, and is thus critical for maintenance of redox balance [16]. In addition to these functions, it has been shown that GSH has effects on MAP kinase signaling and activity of the transcription factor NF-κB [17–19]. Also, it is involved in detoxification of substances in cells, via conjugation and transportation of substances out of cells [20]. Previous studies show that GSH is involved in resistance to some anti-cancer drugs, including cisplatin, doxorubicin, cytosine arabinoside, and daunorubicin [21,22]. γ-GCS is a heterodimer of heavy and light subunits: the catalytic domain is in the heavy subunit; the light subunit is important for regulation of the enzyme activity. Analysis of structure and function of the γ-GCS gene has shown that several cis-elements, including AP-1 and NF-κB binding sites, may be important in expression of this gene, and indicates that ARE is critical for expression of this gene [23].

In the present study, we found that γ-GCSl mRNA levels, GSH concentration, and levels of Nrf2/DNA complex at the ARE of the γ-GCS light subunit (γ-GCSl) gene promoter were higher in the imatinib-resistant BCR/ABL$^+$ cell line KCL22/SR than in the imatinib-sensitive parental cell line KCL22. We also found that ascorbic acid (AA) suppressed migration of Nrf2 to the nucleus, resulting in inhibition of GSH synthesis and restoration of sensitivity to imatinib in KCL22/SR cells.

Materials and methods

Cell culture

KCL22 is a BCR/ABL$^+$ cell line that was established from peripheral blood cells of a patient with CML in BC [24]. KCL22/SR is an imatinib-resistant cell line that was derived from KCL22 in our laboratory [25]. Cells from these lines were grown in RPMI1640 medium supplemented with 10% fetal bovine serum and split every 3 to 4 days. KCL22/SR cells were maintained in the presence of 0.5 mM imatinib. To evaluate effects of GSH on sensitivity of KCL22 cells to imatinib, KCL22 cells were incubated in the presence of 10 mM glutathione monoestel [26] for 24 hours prior to addition of various concentrations of imatinib. An MTT [3-(4,5-dimethylthiazol-2-yl)-2,5-diphenyl tetrazolium bromide] assay was performed to evaluate cytotoxicity, and IC_{50} values were determined from dose-response curves. To examine effects of AA, KCL22/SR cells were cultured without imatinib for 3 days, and were then incubated with 0.5 mM imatinib or 0.125 mM AA for 72 hours. Viable cells were counted by trypan blue exclusion after various periods of incubation.

Determination of glutathione concentration

A total of 2×10^6 cells were harvested and used to assay for glutathione. Glutathione concentration was measured using the GSH-400 system (OXIS Int. Inc., Portland, OR, USA), essentially according to the manufacturer's protocol.

Determination of intracellular peroxides in KCL22/SR cells

Cells were incubated with 2',7'-dichlorofluorescein diacetate (Molecular Probes, Eugene, OR, USA) as the fluorogenic substrate for 30 minutes. The level of intracellular peroxides was determined by flow cytometry, as described previously [27].

RNA blot analysis

Total RNA was isolated from KCL22 and KCL22/SR cells using the acid guanidium thiocyanate–phenol chloroform method [28]. Northern blot analysis was performed as described elsewhere [29]. Human cDNA clones of γ-GCS light and heavy subunits [21] were used as probes. The HG126 clone of the ribosomal RNA gene was used as an internal control.

Western blot analysis

Total cell lysate and nuclear extract were prepared from 1×10^7 cells, using a method described elsewhere [30]. Protein concentration was determined using a Protein Assay Kit (BioRad, Hercules, CA, USA). A 10% polyacrylamide gel was used to separate 10 μg of protein electrophoretically. Immunoblotting and detection by enhanced chemiluminescence were performed as described elsewhere [31]. Rabbit polyclonal anti-Nrf2 (C-20) antibody was purchased from Santa Cruz Biotechnology, Inc. (Santa Cruz, CA, USA). Mouse anti-glyceraldehyde-3-phosphate dehydrogenase monoclonal antibody, which was used as an internal control, was purchased from Chemicon International (Temecula, CA, USA).

DNA gel mobility shift assays

To evaluate the DNA binding activity of Nrf2, DNA gel mobility shift assays were performed using the oligomer 5'-CTACGATTTC-TGCTTAGTCATTGTCTTCC-3', which contains the 11-bp ARE and its flanking sequences. This oligomer was end-labeled with [γ-^{32}P] ATP by T4 polynucleotide kinase (Boehringer Mannheim Corp., Indianapolis, IN, USA). The antisense oligomer was then added to the ^{32}P-end-labeled oligomer to yield a double-stranded probe. Nuclear extracts (5 μg) were incubated with the ^{32}P-labeled oligomer for 15 minutes on ice, in a reaction mixture containing 20 mM HEPES buffer (pH 7.8), 60 mM KCl, 0.2 mM EDTA, 6 mM $MgCl_2$, 0.5 mM dithiothreitol (DTT), 10% [v/v] glycerol and 1.5 μg of an equimolar mixture of poly (dI-dC) and poly (dA-dT). For competition assays, the AREm oligomer 5'-CTACGATTTCTGCTTCGTCCTTGTCTTCC-3', which is a mutated ARE containing two transversions, was used in double-stranded form. In antibody-mediated competition assays, 3 μL of anti-Nrf1, anti-Nrf2, anti-c-Jun, and anti-GATA-2 antibodies (Santa Cruz Biotechnology, Inc., Santa Cruz, CA, USA) were first incubated with nuclear extracts on ice for 20 minutes and were then incubated with the probes for 10 minutes. This mixture was then

loaded onto a 4% polyacrylamide gel and electrophoresed at 150 V and 4°C.

Transfection and luciferase assays

We cotransfected 2 μg of luciferase reporter plasmid fused to human γ-GCSI promoter region (pGCSI-pro; contains ARE and AP-1 binding sites) and 1 μg of effector plasmid or pRL-CMV (internal control) into KCL22/SR cells using TransPast reagent (Promega Corp., Madison, WI, USA), according to the manufacturer's protocol. Briefly, a total of 1×10^6 cells were incubated with the plasmids and TransFast, in 1 mL of medium without serum for 1 hour. Then, 5 mL of fresh medium containing 10% serum was added, and incubation was continued for 48 hours. Luciferase activity was determined using the Dual-Luciferase Reporter Assay System (Promega). Effector plasmids expressing full-length (pcDNA3/mNrf2#0) and dominant-negative (pcDNA3/mNrf2#Eco del) mouse Nrf2 were kindly provided by Drs. K. Ito and M. Yamamoto (Tsukuba University, Tsukuba, Japan).

Results

Formation of Nrf2/DNA complex at ARE was increased in KCL22/SR cells

It has been reported that ARE binds with CNC family transcription factors and plays a critical role in expression of a number of antioxidant and detoxifying enzymes such as γ-GCS, which is a rate-limiting enzyme in GSH synthesis. To clarify whether ARE-mediated regulation of gene expression is involved in imatinib resistance, we first examined DNA binding activity at ARE in the human γ-GCSI gene promoter of KCL22 and KCL22/SR cells using a gel mobility shift assay. The band that was detected was much more prominent in KCL22/SR than in KCL22 (Fig. 1A). This band was completely suppressed by addition of anti-Nrf2 antibody, but not by anti-Nrf1, anti-c-Jun, or anti-GATA-2 antibodies, indicating that it is an Nrf2/DNA complex (Fig. 1B). The increase in Nrf2/DNA complex formation in KCL22/SR cells is not due to increased Nrf2 expression, because there was no difference in Nrf2 protein level between KCL22 and KCL22/SR cells when total cell lysate was used for immunoblot analysis (Fig. 1C). However, when nuclear extracts were used for immunoblot analysis, the level of Nrf2 protein was much higher in KCL22/SR cells than in KCL22 cells (Fig. 1C). These results suggest that induction of Nrf2/DNA complex formation in KCL22/SR cells is caused by movement of Nrf2 from cytoplasm to nucleus.

Nrf2 increased γ-GCS light subunit gene promoter activity

To clarify whether the Nrf2/DNA complex is active in transcription, we examined the effect of Nrf2 on ARE-mediated promoter activation by luciferase reporter assay. Results of these experiments are summarized in Figure 2. When pGCS-pro, which contains ARE and AP-1 sites, was transfected into KCL22/SR cells, luciferase activity increased 150-fold over control activity, which was obtained by transfection of pGL3-Basic promoterless construct. Cotransfection of

Figure 1. Formation of a DNA-protein complex at antioxidant responsive element (ARE) of the human γ-glutamylcystein synthetase light subunit (γ-GCSI) gene promoter. (A): Nuclear extracts (5-mg aliquots) from KCL22 or KCL22/SR cells were incubated with end-labeled oligomers corresponding to ARE. (B): Competition assays were performed with a 200-fold molar excess of the indicated oligonucleotides or anti-Nrf2, anti-Nrf1, anti-c-Jun, and anti-GATA-2 antibodies. (C): Total cell extracts or nuclear extracts were prepared, separated by SDS-polyacrylamide gel electrophoresis, transferred onto a membrane, and reacted with anti-Nrf2 antibody. The expression of glyceraldehyde-3-phosphate dehydrogenase (GAPDH) was examined as an internal control.

the Nrf2 expression vector pcDNA3/Nrf2#0 resulted in a significant increase in luciferase activity. In contrast, expression of the dominant-negative form of Nrf2, which lacks the transcriptional activation domain (pcDNA3/mNrf2#Eco del), suppressed luciferase activity (Fig. 2). These results suggest that ARE in the γ-GCSI gene promoter is active in transcription, and that induction of Nrf2/DNA complex formation at ARE leads to upregulation of promoter activity.

GSH level is higher in KCL22/SR than in KCL22 cells

The level of γ-GCSI mRNA was significantly higher in KCL22/SR cells than in KCL22 cells (Fig. 3A), and the concentration of GSH was 1.5-fold higher in KCL22/SR cells than in KCL22 cells (Fig. 3B). Because γ-GCS is a rate-limiting enzyme of GSH synthesis, upregulation of γ-GCSI

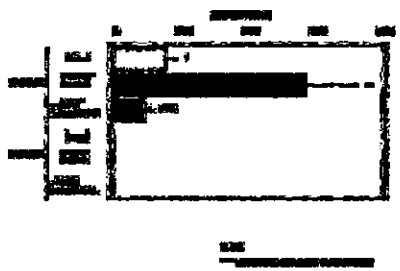

Figure 2. Effect of Nrf2 on the enhancer activity of the human γ-GCSI gene promoter. KCL22/SR cells were transfected with luciferase reporter pGCS-pro or pGL3-Basic together with 1 μg each of pcDNAmNrf2#0 or pcDNA3mNrf2#Eco del effector molecules. Firefly luciferase activity was normalized on the basis of Renilla luciferase activity. The results are expressed as the ratio of firefly luciferase activities of cells transfected with pGL3-basic without any effector molecule.

expression may lead to accumulation of GSH in KCL22/SR cells.

In previous studies, GSH was implicated in resistance to some anti-cancer drugs [9,10]. To clarify whether increased GSH levels are important for resistance to imatinib, we examined the effect of a GSH monoester on sensitivity to imatinib. Addition of a GSH monoester to imatinib-sensitive KCL22 cells resulted in a 2.8-fold increase in the IC_{50} value of imatinib (Fig. 3C). We also examined the effect of buthionine sulfoximine (BSO; a potent inhibitor of γ-GCS) on imatinib sensitivity of KCL22/SR cells, but failed to obtain usable results because of the severe toxicity of BSO.

Ascorbic acid reduced Nrf2/DNA complex formation by inhibiting movement of Nrf2 into nucleus

Because oxidative stress promotes movement of Nrf2 into the nucleus, it is likely that a shift in intracellular redox balance toward a reduced state inhibits movement of Nrf2 in KCL22/SR cells. To verify this hypothesis, we examined the effect of AA (a reducing reagent) on Nrf2/DNA complex formation. Peroxide levels in KCL22/SR cells were reduced by addition of 0.125 mM AA (Fig. 4A), strongly indicating that AA acts as an antioxidant. Formation of Nrf2/DNA complex in KCL22/SR cells was markedly decreased by addition of 0.125 mM AA (Fig. 4B) without any change in Nrf2 protein level in total cell lysate (Fig. 4C), suggesting that AA inhibited movement of Nrf2 into the nucleus.

Ascorbic acid restores imatinib sensitivity in KCL22/SR cells

We next examined the effects of AA on GSH synthesis and growth of KCL22/SR cells. Although the level of γ-GCS heavy subunit mRNA was not changed (data not shown), that of γ-GCSI mRNA was significantly reduced by addition of 0.125 mM AA (Fig. 5A). Simultaneously, GSH concentration in KCL22/SR cells was reduced (Fig. 5B), indicating that AA inhibited GSH synthesis. AA had no inhibitory effect on

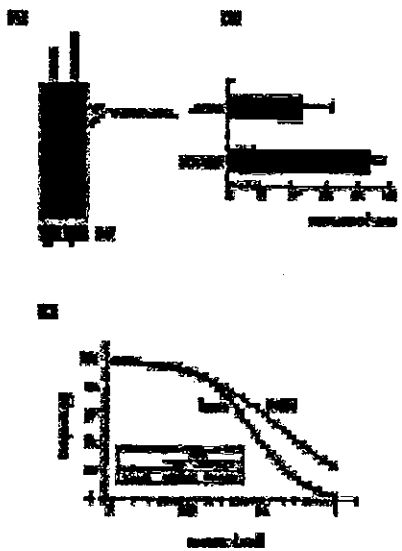

Figure 3. Glutathione synthesis in KCL22/SR cells. (A): The levels of γ-GCSI mRNA were analyzed by Northern blotting. The filter was rehybridized to a ribosomal RNA probe. 28S ribosomal RNA bands are shown. (B): Glutathione (GSH) concentration was measured with the GSH-400 system (OXIS Int. Inc.), using 2×10^6 KCL22 or KCL22/SR cells, as described in Materials and Methods. (C): KCL22 cells were cultured with various concentrations of imatinib for 72 hours in the presence or absence of GSH. The ratio of IC_{50} is shown in the figure.

growth of KCL22/SR cells when administered alone, but combined treatment of KCL22/SR cells with imatinib and AA resulted in inhibition of cell growth (Fig. 5C). Consistent with these findings, addition of 0.125 mM AA resulted in a 50% decrease in the IC_{50} value of imatinib for KCL22/SR cells, suggesting that AA at this concentration is not directly cytotoxic but restores sensitivity of KCL22/SR cells to imatinib via, at least in part, suppression of intracellular GSH level.

Formation of Nrf2/DNA complex is increased in another imatinib-resistant cell line

To clarify whether an increase in formation of Nrf2/DNA complex occurs in imatinib-resistant cells in general or occurs only in KCL22/SR cells, we performed gel mobility shift assays using nuclear extracts of the imatinib-resistant cell lines K562/SR and KU812/SR, which were recently cloned in our lab, and their imatinib-sensitive parental strains (K562 and KU812, respectively). As shown in Figure 6, while there was no difference in the level of Nrf2/DNA complex between KU812/SR and KU812, the level of Nrf2/DNA complex was higher in K562/SR than in K562. These

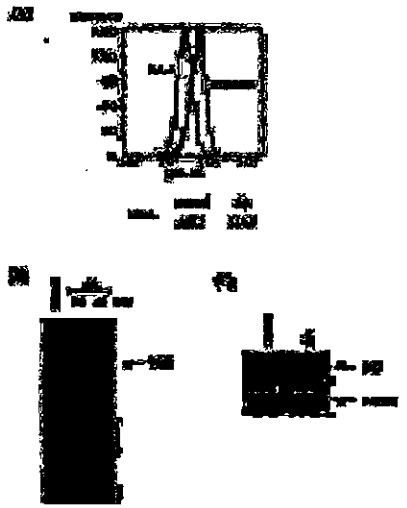

Figure 4. Effect of ascorbic acid on formation of Nrf2/DNA complex. (A): KCL22/SR cells were incubated with 0.125 mM ascorbic acid (AA) for 6 hours. The level of intracellular peroxides was determined by flow cytometry, as described in Materials and Methods. Decreased green fluorescence correlates with decreased peroxide levels. (B): KCL22/SR cells were incubated with 0.125 mM AA. The level of Nrf2/DNA complex formation at various time points was evaluated by gel mobility shift assay using oligomers corresponding to ARE. (C): KCL22/SR cells were cultured in the absence or presence of 0.125 mM AA for 24 hours. The levels of Nrf2 protein in total cell extracts were examined by immunoblot analysis using anti-Nrf2 antibody. The expression of glyceraldehyde-3-phosphate dehydrogenase (GAPDH) was examined as an internal control.

results suggest that induction of Nrf2 activity is involved in resistance to imatinib in some, but not all, imatinib-resistant cell lines.

Discussion

Recently, various new anti-cancer agents that target specific oncogenic molecules have been developed. Imatinib is one of the most successful of these reagents. However, a major problem with imatinib treatment is acquisition of resistance. In the present study, we used the imatinib-resistant BCR/ABL$^+$ cell line KCL22/SR to investigate the mechanisms of resistance to imatinb. KCL22/SR was cloned from the human BCR/ABL$^+$ cell line KCL/22. The IC_{50} value of imatinib for KCL22/SR is about 11.6-fold higher than that of KCL22, indicating that KCL22/SR has acquired significant resistance to imatinib [25]. Examination of KCL22/SR has revealed no mutations in the BCR/ABL gene and no increase in levels of BCR/ABL protein or P-glycoprotein. Given that the level of phosphorylated BCR/ABL protein is suppressed by imatinib treatment, these previous findings suggest that mechanisms independent of BCR/ABL activity are involved in the imatinib resistance of KCL22/SR [25]. The present results suggest that Nrf2 is involved in the imatinib resistance of KCL22/SR.

Nrf2 has been shown to regulate ARE-mediated gene expression. The present results demonstrate that formation of Nrf2/DNA complex at the ARE of the γ-GCSl gene promoter occurs at a significantly higher rate in KCL22/SR cells than in KCL22 cells (Fig. 1A). The amount of Nrf2/DNA complex was also increased in the imatinib-resistant cell line K562/SR, compared with its parental imatinib-sensitive line, K562 (Fig. 6), suggesting that this phenomenon occurs in many types of imatinib-resistant cells other than KCL22/SR cells. Consistent with these findings, the level of γ-GCSl mRNA was significantly higher in KCL22/SR cells than in KCL22 cells (Fig. 3A). The light subunit of the γ-GCS enzyme is a regulatory subunit and is important for regulation of γ-GCS activity. There was no difference in levels of γ-GCS heavy subunit (which contains a catalytic domain of γ-GCS) mRNA between KCL22/SR and KCL22 (data not shown). Nrf2-mediated induction of light subunit expression may result in upregulation of γ-GCS activity and a consequent increase in GSH synthesis (Fig. 3B). Addition of a GSH monoester to KCL22 cells resulted in an increase in the IC_{50} value of imatinib (Fig. 3C), suggesting that upregulation of GSH synthesis due to increased Nrf2 activity is involved, at least in part, in the imatinib resistance of KCL22/SR cells. Clarification of whether similar abnormalities are involved in the imatinib resistance in primary cells from imatinib-resistant leukemia patients is important, and such studies are now being carried out in our laboratory.

GSH has been shown to detoxify substances in cells via conjugation and transport out of the cell [20]. However, it is unlikely that GSH directly inactivates imatinib via conjunction in KCL22/SR cells, because imatinib still effectively suppressed BCR/ABL kinase activity in these cells. Thus, mechanisms of imatinib resistance due to GSH accumulation may involve effects on other biological functions, such as intracellular signaling. Since addition of GSH did not result in restoration of the imatinib-mediated reduction of phospho-ERK1/2 levels in KCL22 cells (data not shown), MAPK may not be involved in the mechanisms of imatinib resistance due to GSH accumulation.

The present findings strongly suggest that Nrf2 is a good molecular target for overcoming imatinib resistance. AA reduced peroxide levels (Fig. 4A) and suppressed levels of Nrf2/DNA complex at the ARE of the γ-GCSl gene promoter (Fig. 4B). Consistent with these results, treatment of KCL22/SR cells with AA resulted in reduced GSH level and enhanced sensitivity to imatinib (Fig. 5C). Although we have no clinical data on the effect of ascorbic acid in imatinib-resistant patients, an in vitro experiment showed that treatment with AA and imatinib also suppressed growth of leukemia cells from a patient with CML in BC who had relapsed during

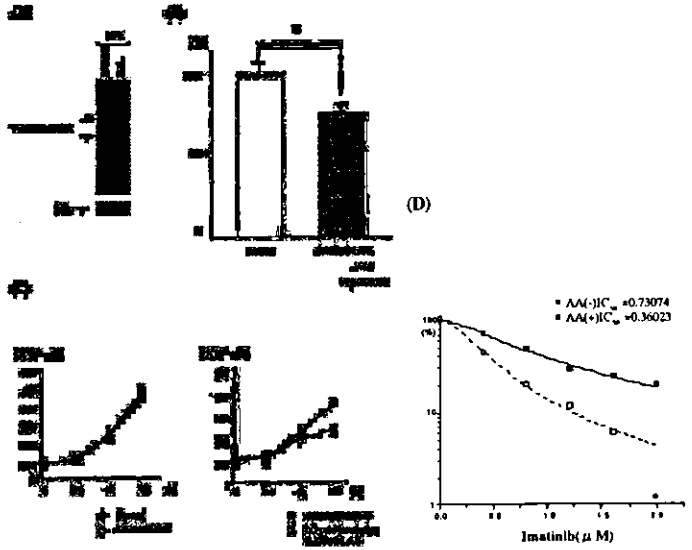

Figure 5. Effect of AA on GSH synthesis in KCL22/SR cells. (A,B): KCL22/SR cells were cultured in the presence of 0.125 mM AA for 24 hours. Changes in the levels of γ-GCSl mRNA (A) and GSH concentration (B) were examined as described in Materials and Methods. (C): KCL22/SR cells were incubated with or without 0.125 mM AA in the absence or presence of 0.5 μM imatinib for 72 hours. Viable cells were counted by trypan blue exclusion at various time points, as indicated in the figure. (D): KCL22/SR cells were incubated in the presence of various concentrations of imatinib with or without ascorbic acid. The IC_{50} values of imatinib are shown in the figure.

Figure 6. Formation of Nrf2/DNA complex at ARE in other imatinib-resistant cell lines. Nuclear extracts were prepared from K562, K562/SR, KU812, and KU812/SR cells. Gel mobility shift assay was performed using the end-labeled oligomers corresponding to ARE.

imatinib treatment (data not shown). We did not examine changes in Nrf2/DNA complex formation induced by AA in that case; however, it is possible that AA-induced inhibition of Nrf2 activity strengthened the effect of imatinib. It has been reported that reactive oxygen species could inhibit the activity of protein tyrosine phosphatases, resulting in the induction of protein tyrosine phosphorylation [32]. Thus, AA may also have other biological effects through phosphatase activation. Taken together, these results suggest that AA is an attractive molecular target reagent for overcoming resistance to imatinib in some imatinib-resistant CML cells.

Acknowledgments

This work was supported in part by Grants-in-Aid from the Ministry of Education, Culture, Sports, Science and Technology, Japan. We wish to thank Ms. E. Yamakawa for her help in preparation of the manuscript.

References

1. Druker BJ, Talpaz M, Resta DJ, et al. Efficacy and safety of a specific inhibitor of the BCR-ABL tyrosine kinase in chronic myeloid leukemia. N Engl J Med. 2001;344:1031–1037.

2. Druker BJ, Sawyers CL, Kantarjian H, et al. Activity of a specific inhibitor of the BCR/ABL tyrosine kinase in the blast crisis of chronic myeloid leukemia and acute lymphoblastic leukemia with the Philadelphia chromosome. N Engl J Med. 2001;344:1038–1042.
3. Sawyers CL, Hochhaus A, Feldman E, et al. Imatinib induces hematologic and cytogenetic responses in patients with chronic myelogenous leukemia in myeloid blast crisis: results of a phase II study. Blood. 2002;99:3530–3539.
4. le Coutre P, Tassi E, Varella-Garcia M, et al. Induction of resistance to the Abelson inhibitor STI571 in human leukemic cells through gene amplification. Blood. 2000;95:1758–1766.
5. Weisberg E, Griffin JD. Mechanism of resistance to the ABL tyrosine kinase inhibitor STI571 in BCR/ABL-transformed hematopoietic cell lines. Blood. 2000;95:3498–3505.
6. Mahon FX, Deininger MW, Schultheis B, et al. Selection and characterization of BCR-ABL$^+$ cell lines with differential sensitivity to the tyrosine kinase inhibitor STI571: diverse mechanisms of resistance. Blood. 2000;96:1070–1079.
7. Gorre ME, Mohammed M, Ellwood K, et al. Clinical resistance to STI571 cancer therapy caused by BCR-ABL gene mutation of amplification. Science. 2001;293:876–880.
8. Branford S, Rudzki Z, Walsh S, Grigg A, Arthur C, Taylor K. High frequency of point mutations clustered within the adenosine triphosphate–binding region of BCR/ABL in patients with chronic myeloid leukemia or Ph$^+$ acute lymphoblastic leukemia who develop imatinib (STI571) resistance. Blood. 2002;99:3472–3475.
9. Gambacorti-Passerini C, Barni R, le Coutre P, et al. Role of α1 acid glycoprotein in the in vivo resistance of human BCR-ABL$^+$ leukemic cells to the Abl inhibitor STI571. J Natl Cancer Inst. 2000;92:1641–1650.
10. Venugopal R, Jaiswal AK. Nrf1 and Nrf2 positively and c-Fos and Fra1 negatively regulate the human antioxidant response element–mediated expression of NAD(P)H:quinone oxidoreductase1 gene. Proc Natl Acad Sci U S A. 1996;93:14960–14965.
11. Venugopal R, Jaiswal AK. Nrf2 and Nrf1 in association with Jun proteins regulate antioxidant response element–mediated expression and coordinated induction of genes encoding detoxifying enzymes. Oncogene. 1998;17:3145–3156.
12. Itoh K, Wakabayashi N, Katoh Y, et al. Keap1 represses nuclear activation of antioxidant responsive elements by Nrf2 through binding to the amino-terminal Neh2 domain. Genes Dev. 1999;13:76–86.
13. Itoh K, Chiba T, Takahashi S, et al. An Nrf2/small Maf heterodimer mediates the induction of phase II detoxifying enzyme genes through antioxidant response elements. Biochem Biophys Res Commun. 1997; 236:313–322.
14. Ishii T, Itoh K, Takahashi S, et al. Transcription factor Nrf2 coordinately regulates a group of oxidative stress-inducible genes in macrophages. J Biol Chem. 2000;275:16023–16029.
15. Richman PG, Meister A. Regulation of γ-glutamyl-cysteine synthetase by nonallosteric feedback inhibition by glutathione. J Biol Chem. 1975; 250:1422–1426.
16. Meister A. Glutathione metabolism. Methods Enzymol. 1995;251:3–7.
17. Filomeni G, Rotilio G, Ciriolo MR. Glutathione disulfide induces apoptosis in U937 cells by a redox-mediated p38 MAP kinase pathway. FASEB J. 2003;17:64–66.
18. Kong AN, Yu R, Lei W, Mandlekar S, Tan TH, Ucker DS. Differential activation of MAPK and ICE/Ced-3 protease in chemical-induced apoptosis: the role of oxidative stress in the regulation of mitogen-activated protein kinases (MAPKs) leading to gene expression and survival or activation of caspases leading to apoptosis. Restor Neurol Neurosci. 1998;12:63–70.
19. Haddad JJ. Redox regulation of pro-inflammatory cytokines and IκB-α/NF-κB nuclear translocation and activation. Biochem Biophys Res Commun. 2002;296:847–856.
20. Hayes JD, Pulford DJ. The glutathione S-transferase supergene family: regulation of GST and the contribution of the isoenzymes to cancer chemoprotection and drug resistance. Crit Rev Biochem Mol Biol. 1995;30:445–600.
21. Iida T, Mori E, Mori K, et al. Co-expression of γ-glutamylcysteine synthetase sub-units in response to cisplatin and doxorubicin in human cancer cells. Int J Cancer. 1999;82:405–411.
22. Takemura H, Urasaki Y, Yoshida A, Fukushima T, Ueda T. Simultaneous treatment with 1-β-D-arabinofuranosylcytosine and daunorubicin induces cross-resistance to both drugs due to a combination-specific mechanism in HL60 cells. Cancer Res. 2001;61:172–177.
23. Moinova HR, Mulcahy RT. An electrophile responsive element (EpRE)regulates β-naphthoflavone induction of the human γ-glutamylcysteine synthetase regulatory subunit gene. Constitutive expression is mediated by an adjacent AP-1 site. J Biol Chem. 1998;273:14683–14689.
24. Kubonishi I, Miyoshi I. Establishment of a Ph1 chromosome–positive cell line from chronic myelogenous leukemia in blast crisis. Int J Cell Cloning. 1983;1:105–117.
25. Ohmine K, Nagai T, Tarumoto T, et al. Analysis of gene expression profiles in an imatinib-resistant cell line, KCL22/SR. Stem Cells. 2003; 21:315–321.
26. Anderson ME, Levy EJ, Meister A. Preparation and use of glutathione monoesters. Methods Enzymol. 1994;234:492–499.
27. Nagai T, Tarumoto T, Miyoshi T, et al. Oxidative stress is involved in hydroxyurea-induced erythroid differentiation. Br J Haematol. 2003; 121:657–661.
28. Chomczynski P, Sacchi N. Single-step method of RNA isolation by acid guanidinium thiocyanate-phenol-chloroform extraction. Anal Biochem. 1987;162:156–159.
29. Nagai T, Harigae H, Ishihara H, et al. Transcription factor GATA-2 is expressed in erythroid, early myeloid, and CD34$^+$ human leukemia–derived cell lines. Blood. 1994;84:1074–1084.
30. Lassar AB, Davis RL, Wright WE, et al. Functional activity of myogenic HLH proteins requires hetero-oligomerization with E12/E47-like proteins in vivo. Cell. 1991;66:305–315.
31. Nagai T, Harigae H, Furuyama K, et al. 5-aminolevulinate synthase expression and hemoglobin synthesis in a human myelogenous leukemia cell line. J Biochem (Tokyo). 1997;121:487–495.
32. Sattler M, Verma S, Shrikhande G, et al. The BCR/ABL tyrosine kinase induces production of reactive oxygen species in hematopoietic cells. J Biol Chem. 2000;275:24273–24278.

Available online at www.sciencedirect.com
SCIENCE DIRECT
Biochemical and Biophysical Research Communications 329 (2005) 1343–1349
BBRC
www.elsevier.com/locate/ybbrc

Overexpression of calreticulin sensitizes SERCA2a to oxidative stress

Yoshito Ihara [a,b,*], Kan Kageyama [a], Takahito Kondo [a]

[a] Department of Biochemistry and Molecular Biology in Disease, Atomic Bomb Disease Institute, Nagasaki University Graduate School of Biomedical Sciences, Nagasaki 852-8523, Japan
[b] CREST, JST Kawaguchi 332-1102, Japan

Received 9 February 2005

Abstract

Calreticulin (CRT), a Ca^{2+}-binding molecular chaperone in the endoplasmic reticulum, plays a vital role in cardiac physiology and pathology. Oxidative stress is a main cause of myocardiac disorder in the ischemic heart, but the function of CRT under oxidative stress is not fully understood. In this study, the effect of overexpression of CRT on sarcoplasmic/endoplasmic reticulum Ca^{2+}-ATPase (SERCA) 2a under oxidative stress was examined using myocardiac H9c2 cells transfected with the CRT gene. The in vitro activity of SERCA2a and uptake of $^{45}Ca^{2+}$ into isolated microsomes were suppressed by H_2O_2 in CRT-overexpressing cells compared with controls. Moreover, SERCA2a protein was degraded via a proteasome-dependent pathway following the formation of a complex with CRT under the stress with H_2O_2. Thus, we conclude that overexpression of CRT enhances the inactivation and degradation of SERCA2a in the cells under oxidative stress, suggesting some pathophysiological functions of CRT in Ca^{2+} homeostasis of myocardiac disease.

Keywords: Calreticulin; Chaperone; Endoplasmic reticulum; Oxidative stress; SERCA

Calreticulin (CRT) is a Ca^{2+}-binding molecular chaperone expressed in the endoplasmic reticulum (ER) of a wide variety of eukaryote cells [1]. CRT is involved in many biological processes including the regulation of Ca^{2+} homeostasis [2] and intracellular signaling, cell adhesion, gene expression, glycoprotein folding [3,4], and nuclear transport [5]. CRT is well expressed in embryonic rat heart but its expression is suppressed after birth [6]. It has been shown that CRT is essential for cardiac development in mice [7,8]. CRT-deficient embryonic cells showed an impaired nuclear import of nuclear factor of activated T cell (NF-AT3), a transcription factor, indicating that CRT functions in cardiac development as a component of the Ca^{2+}/calcineurin/NF-AT/GATA-4 transcription pathway [7]. On the other hand, CRT transgenic mice suffer a complete heart block and sudden death [9]. The CRT-dependent cardiac block involves an impairment of both the L-type Ca^{2+} channel and gap junction connexins (Cx40 and Cx43). CRT is also over-expressed in rat cardiomyocytes under pressure-overload cardiac hypertrophy, implying some dysfunction of cardiomyocytes related with the overexpression [10]. Furthermore, in cultured myocardiac H9c2 cells, overexpression of CRT following gene transfection promoted apoptosis during cardiac differentiation [11]. These studies suggest that CRT plays a vital role in myocardiac development and function, though how has not been fully clarified.

Sarcoplasmic/endoplasmic reticulum Ca^{2+}-ATPase (SERCA) is an integral membrane protein of the ER or SR that catalyzes the ATP-dependent transport of Ca^{2+} from the cytosol to the lumen of ER or SR [12]. SERCA in the heart plays a pivotal role in the beating function of the heart. SERCA promotes muscle relaxation by lowering the cytosolic Ca^{2+} concentration and through active Ca^{2+} transport restores the intracellular Ca^{2+} stores, thus providing Ca^{2+} needed for the next contraction. Decreases in SERCA pump expression and activity have been observed in a variety of pathological conditions of the heart [13]. Oxidative stress with reactive oxygen species generated during ischemia and reperfusion is implied in the mechanism for cardiac damage [14]. SERCA is also known to be sensitive to oxidative stress, such as hydroxyl radical, peroxide, and peroxynitrite [15–17]. Inactivation of SERCA by oxidative stress may be implicated in dysfunction of myocardiac cells under the stress.

In *Xenopus* oocytes, it was reported that CRT inhibits Ca^{2+} oscillation enhanced by SERCA2b through the lectin function of CRT [18–21]. Baker et al. [22] have also reported the functional interaction between CRT and SERCA in cultured HeLa cells. However, the pathophysiological significance of CRT expression levels and SERCA functions in cardiomyocytes under oxidative stress has not been revealed. Here we investigated the biological role of CRT using rat myocardiac H9c2 cells transfected with the CRT gene. We first show that overexpression of CRT enhances the inactivation and degradation of SERCA2a via increased interaction with CRT under oxidative stress.

Materials and methods

Materials. Antibodies against CRT (C-terminal), calnexin (CNX), and BiP/Grp78 were purchased from Stressgen (Victoria, BC, Canada). The goat antibody against CRT (N-terminal) was obtained from Santa Cruz Biotechnology (Santa Cruz, CA). The monoclonal antibody against SERCA2 (clone 2A7-A1) was obtained from Sigma (St. Louis, MO). Peroxidase-conjugated secondary antibodies against IgG of rabbit and mouse were from Dako (Denmark). The other reagents used in the study were all of high grade, from Sigma or Wako Pure Chemicals (Osaka, Japan).

Cell lines and culture. H9c2 cells, a clonal line derived from embryonic rat heart, were obtained from American Type Culture Collection (CRL-1446). H9c2 cells which had been transfected with the expression vector for mouse CRT cDNA have been described previously [11]. A cell line (CRT-S8) expressing high level of CRT protein was used in the study. A 0.6-kbp restriction fragment with *Eco*RI, containing the translation initiation site, was cut out from the vector pcDNA3.1/mCRT [11] and inserted in the reverse orientation in pcDNA3.1 (Invitrogen) to obtain an antisense CRT. The antisense cDNA expression vector was also transfected into H9c2 cells to establish a cell line (CRT-AS) in which the expression of CRT was suppressed. Cells were cultured in Dulbecco's modified Eagle's medium, supplemented with 10% fetal calf serum under a humidified atmosphere of 95% air and 5% CO_2 at 37 °C. To induce oxidative stress, cells were cultured with the medium containing different concentrations of H_2O_2.

Immunoprecipitation and immunoblot analysis. Cultured cells were harvested and lysed in lysis buffer [20 mM Tris-HCl (pH 7.2), 130 mM NaCl, and 1% NP-40 including protease inhibitors (20 μM APMSF, 50 μM pepstatin, and 50 μM leupeptin)]. Cell lysates normalized for protein levels were immunoprecipitated using the primary antibodies. After preclearing, the cell lysates were incubated with the primary antibodies at 4 °C for 2 h followed by another 1 h with protein G-Sepharose beads (Amersham Biosciences). For immunoblot analysis, proteins were eluted from the beads by boiling with SDS-dye solution after a wash with the lysis buffer. Protein samples were electrophoresed on 7.5 or 10% SDS-polyacrylamide gels under reducing conditions and then transferred to nitrocellulose membrane as described before [23].

The membrane was blocked with 5% skim milk in TBS [10 mM Tris-HCl (pH 7.5) and 150 mM NaCl] and then incubated at 4 °C overnight with the primary antibody in TBS containing 0.05% Tween 20. The blots were coupled with the peroxidase-conjugated secondary antibodies, washed, and then developed using the ECL chemiluminescence detection kit (Amersham Biosciences) according to the manufacturer's instructions.

Assays of Ca^{2+}-ATPase and Ca^{2+} uptake in the microsomes. For the preparation of microsome, cultured cells were homogenized with homogenization buffer [10 mM Hepes (pH 7.4), 150 mM KCl, 250 mM sucrose, and protease inhibitors]. Homogenates were centrifuged at 1000*g* for 20 min at 4 °C, and then the supernatant was centrifuged at 10,000*g* for 20 min at 4 °C. Supernatants were recovered and ultracentrifuged at 105,000*g* for 60 min at 4 °C. The pellet was resuspended in the homogenization buffer and centrifuged again for 60 min. The final pellet was suspended in the homogenization buffer to obtain a protein concentration of 0.5 mg/ml and stored as a small aliquot at −80 °C. The microsomes were incubated with different concentrations of H_2O_2 for 30 min at 37 °C, and then ATPase and Ca^{2+} uptake activities were determined. Ca^{2+}-dependent ATPase activities were determined spectrophotometrically for untreated and H_2O_2-treated microsomes according to the methods described by Favero et al. [24]. Assays were conducted at 22 °C with 80 μg of microsomal protein in 1 ml of the assay buffer [20 mM Hepes (pH 7.0), 100 mM KCl, 1 mM $MgCl_2$, 1 mM EGTA, 3 mM NADH, 1 mM phosphoenolpyruvate, lactate dehydrogenase (5 U), pyruvate kinase (5 U), and 0.5 mM Mg-ATP]. At first, Ca^{2+}-independent (Mg^{2+}-dependent) ATPase activity was initiated by the addition of the microsome sample to the cuvette, and the change of absorbance at 340 nm was monitored for 2 min. Then, Ca^{2+}-dependent ATPase activity was measured by adding $CaCl_2$ to a final concentration of 10 μM, and again the change of absorbance was monitored for 3 min. The ATPase activity was evaluated from the falling rate of NADH absorbance at 340 nm. Ca^{2+} uptake was measured radiometrically using the Millipore filtration technique as described previously [25] with a slight modification. Assays were conducted on ice with 80 μg of microsomal protein in 90 μl Ca^{2+} uptake buffer consisting of 10 mM Hepes (pH 7.4), 150 mM KCl, 250 mM sucrose, 10 μM ATP, and 1 μCi $^{45}CaCl_2$. The aliquots were incubated on ice for 5 min, and the reaction was terminated by adding 20 μl of 50 mM EGTA and 125 mM $MgCl_2$. Aliquots were filtered through a 0.45-μm nitrocellulose filter under vacuum conditions. The filters were rinsed twice with 0.5 ml of washing buffer [10 mM Hepes (pH 7.4), 150 mM KCl, 2 mM EGTA, and 2.5 mM $MgCl_2$]. $^{45}Ca^{2+}$ uptake was calculated by measuring the radioactivity and standardized using protein concentrations. The data are represented as a percentage of untreated controls.

Fluorescence microscopy. Cells (50,000 per ml) were grown on Lab-Tek chamber slides (Nunc) for 24 h. They were fixed with 4% paraformaldehyde in phosphate-buffered saline (PBS; pH 7.2) and permeabilized for 10 min with PBS containing 1% Triton X-100. The cells were then blocked with 1% BSA in PBS, incubated with the antibody for 1 h, and washed with PBS containing 1% BSA. The immunoreactive primary antibodies were visualized with fluorescein isothiocyanate (FITC)-conjugated anti-rabbit immunoglobulins (Cappel) or rhodamine-conjugated anti-mouse immunoglobulins (Dako). After a wash, the stained cells were mounted in the Vectashield medium. A Zeiss Axioskop2 (Carl Zeiss, Jena, Germany), with epi-illumination for fluorescence, was used for the fluorescence microscopic analysis.

* Corresponding author. Fax: +81 95 849 7100.
E-mail address: y-ihara@net.nagasaki-u.ac.jp (Y. Ihara).

0006-291X/$ - see front matter © 2005 Elsevier Inc. All rights reserved.
doi:10.1016/j.bbrc.2005.02.112

Results

Overexpression CRT enhances the inactivation of SERCA2a in vitro under oxidative stress with H_2O_2

Rat myocardiac H9c2 cells were transfected with the sense and antisense CRT gene expression vectors to obtain cell lines overexpressing and underexpressing CRT, respectively. Fig. 1A shows that the expression of CRT increased in the overexpresser (CRT-S8) to approximately 270% of the level in the parental and mock-transfected (control) H9c2 cells. In the underexpresser (CRT-AS), the expression of CRT was decreased to approximately 30% of the control level. The transfection had no apparent effect on the expression of other ER proteins such as CNX and BiP. Under oxidative stress, a variety of cellular proteins are known to be oxidized and inactivated [26]. SERCA2 is one protein highly susceptible to the stress [15–17]. To examine how the expression level of CRT influences the function of SERCA2a under stress due to H_2O_2, the effect of H_2O_2 treatment on SERCA2a activity was examined in vitro using microsomes isolated from control, CRT-overexpressing, and CRT-underexpressing cells. The microsomes were prepared from cells, treated with different concentrations of H_2O_2 (0–200 μM) for 30 min, and then assayed for SERCA activity as described in Materials and methods. As shown in Fig. 1B, the activity was suppressed after 30-min treatment with H_2O_2 in a dose-dependent manner, and the inactivation was enhanced in CRT-overexpressing cells compared to controls, but was suppressed in CRT-underexpressing cells compared to controls. It was also noteworthy that the expression levels of CRT had less influence on the basal level of SERCA activity in the microsomes of untreated cells. To confirm whether the inactivation of SERCA reflects the loss of Ca^{2+} pumping function, $^{45}Ca^{2+}$ uptake into microsomes was also examined in vitro under the conditions. The microsomes were treated for 30 min with H_2O_2 as described above, and then $^{45}Ca^{2+}$ uptake into microsomes was measured as described in Materials and methods. As shown in Fig. 1C, the uptake of $^{45}Ca^{2+}$ was suppressed by H_2O_2 treatment in a dose-dependent manner, and the suppression was enhanced in CRT-overexpressing cells compared with controls, but was suppressed in CRT-underexpressing cells compared

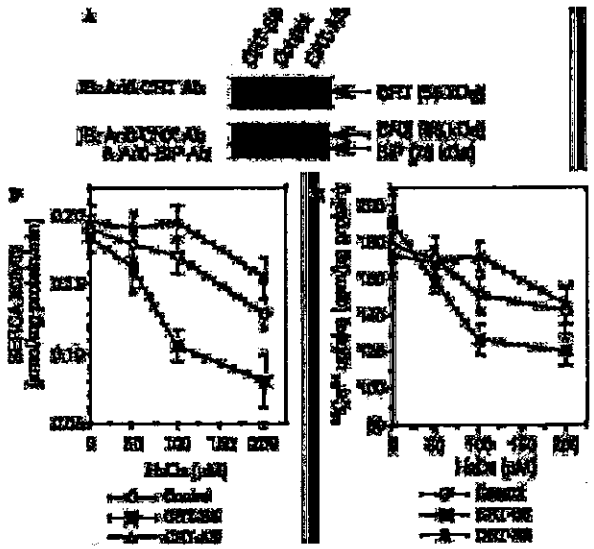

Fig. 1. The expression level of CRT influences the H_2O_2-induced inactivation of SERCA2a and $^{45}Ca^{2+}$ uptake in isolated microsomes in vitro. (A) The expression levels for CRT, CNX, and BiP were estimated in mock-transfected (control), CRT-overexpressing (CRT-S8), and CRT-underexpressing (CRT-AS) cells by immunoblot analysis using specific antibodies as described in Materials and methods. To estimate the effect of H_2O_2 on SERCA2a activity and $^{45}Ca^{2+}$ uptake in isolated microsomes in vitro, microsomes were isolated from control, CRT-overexpressing, and CRT-underexpressing cells as described in Materials and methods. Microsomes were treated with different concentrations of H_2O_2 for 30 min, and then SERCA activity (B) and $^{45}Ca^{2+}$ uptake (C) were measured as described in Materials and methods. Each value represents the mean ± SD of three independent experiments.

with controls. Taken together, overexpression of CRT enhances inactivation of SERCA2a following treatment with H_2O_2, leading to an enhanced suppression of Ca^{2+} uptake into the microsomes. In contrast, suppression of CRT expression prevents the inactivation of SERCA2a following the treatment with H_2O_2.

Overexpression of CRT enhances the degradation of SERCA2a in H9c2 cells under oxidative stress with H_2O_2

To further know the effect of oxidative stress on SERCA2a in CRT-overexpressing cells, the change in the protein level of SERCA2a in whole cells was examined by immunoblot analysis in control and gene-transfected cells during oxidative stress with H_2O_2. Fig. 2A shows

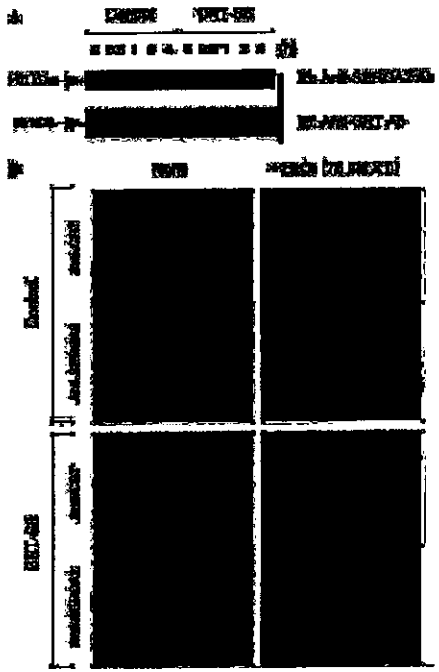

Fig. 2. The expression level of SERCA2a is decreased in CRT-overexpressing H9c2 cells under oxidative stress. (A) Control and CRT gene-transfected (CRT-S8) cells were treated with H_2O_2 (75 μM) for the indicated periods. The expression levels for SERCA2a and CRT were examined by immunoblot analysis using specific antibodies as described in Materials and methods. (B) Control and CRT gene-transfected (CRT-S8) cells were treated with H_2O_2 (75 μM) for 2 h. The intracellular localization of SERCA2a and CRT was examined by immunofluorescence (IF) microscopy using specific antibodies as described in Materials and methods.

that the protein level of SERCA2a apparently decreases 1 h after the treatment with 75 μM H_2O_2 in the gene-transfected cells, with a slight change in control cells. The intracellular localization of SERCA2a was also characterized by immunofluorescence microscopy in control and gene-transfected cells treated with or without 75 μM H_2O_2 for 2 h (Fig. 2B). In control cells, immunoreactivity for SERCA2a showed a perinuclear localization and vesicular pattern, similar to that of CRT, and showed no apparent change after H_2O_2 treatment. On the other hand, CRT was diffusively distributed in the cytoplasm and nucleus after H_2O_2 treatment, although the signal intensity was not diminished by the treatment. In contrast, in the case of gene-transfected cells, damaged cells were round and shrunk with some bleb-like structure, and intracellular compartments seemed destroyed by H_2O_2. Intracellular localization of the signals also showed a diffusive pattern compared to that of untreated cells for both CRT and SERCA2a. Together, in the gene-transfected cells treated with H_2O_2, the structure of intracellular compartments such as ER was apparently destroyed, and the intracellular localization of both CRT and SERCA2a was influenced. Moreover, it was noteworthy that the total cellular level of SERCA2a was apparently decreased in gene-transfected cells during the H_2O_2 treatment, whereas no decrease was seen in that of CRT.

The interaction of CRT with SERCA2a is enhanced in CRT-overexpressing H9c2 cells under oxidative stress with H_2O_2

To investigate whether CRT interacts with SERCA2a under oxidative stress, SERCA2a was immunoprecipitated with the anti-SERCA2 antibody from cell lysates after treatment with H_2O_2 (75 μM) for various periods, and then the immunoprecipitates were subjected to immunoblot analysis using the anti-CRT antibody. As shown in Fig. 3A, CRT was coimmunoprecipitated with the anti-SERCA2 antibody from control cells treated with H_2O_2 for 15 min. The interaction diminished after 30-min treatment with H_2O_2, indicating that CRT transiently interacted with SERCA2a under oxidative stress. On the other hand, CRT was coimmunoprecipitated with anti-SERCA2 antibody from untreated CRT-overexpressing cells. The interaction increased slightly during 60-min treatment with H_2O_2, although the total amount of immunoprecipitated SERCA2a gradually decreased. Conversely, CRT was immunoprecipitated with the specific antibody from cell lysates after treatment with H_2O_2 (75 μM) for various periods, and then the immunoprecipitates were subjected to immunoblot analysis using the anti-SERCA2 antibody. As shown in Fig. 3B, SERCA2a was coimmunoprecipitated with the anti-CRT antibody from control cells treated with H_2O_2 for 15 min. The interaction diminished after 30-min treatment with H_2O_2. This